THE ELECTRIC-STREAMING BIREFRINGENCE METHOD

by

Yasuo MUKOHATA

Contents

SUMMARY

A new method which permits the simultaneous determination of the rotational diffusion constant and the elctrical and optical properties of colloidal macromolecules is designated "the electric-streaming birefringence method". With this method, the rotational diffusion behavior of colloidal macromolecules under the influence of two externally applied orientation fields, an electrostatic one and a velocity gradient of streaming medium are solved theoretically.

The theoretical treatment compared the present method with the more clearly defined cases of streaming birefringence and electric birefringence. The comparison was found suitable when the strengths of the two externally applied fields are small.

An apparatus suitable for determining electric-streaming birefringence was constructed by modifying a streaming birefringence apparatus of the concentric cylinder type.

Certain experiments were made with a m-cresol solution of poly-γ-benzyl-L-glutamate (PBLG). From the results, it was possible to calculate the residual permanent dipole moment of PBLG which was 3.4D, and this is in satisfactory agreement with the well-known value for the peptide bond moment.

By the utilization of a rapid and accurate photographing technique to determine the extinction angle, which was found to be more sensitive to the applied electric field than the magnitude of birefringence, it was possible to shorten the duration of the experiments. A photographing technique thus minimizes the probability of unexpected effects on the solution being

studied during the application of the electric field.

Some experiments were also made with an alternating electric field in conjunction with a hydrodynamic field. With increasing frequency the extinction angle of PBLG in m-cresol deviated from the value obtained with an electrostatic field of the same effective strength; at higher frequencies the value was equal to that found without an electric field.

However, this frequency dependent deviation of the value of the extinction angle was not found in the experiments carried out with yellow bentonite suspended in 95% aqueous glycol.

These frequency dependence (orientation dispersion) experiments, employing alternating electric fields, provide an excellent method to discriminate between individual values of the permanent and the induced dipole moments of macromolecules.

I Introduction

Rotational Brownian movement of colloidal particles are less spectacular than translational movement when observed under the microscope, although they have been successfully observed by Perrin (1). There are many physico-chemical phenomena related to the rotational diffucion of colloidal macromolecules dispersed in a suspending medium such as Maxwell and Kerr effects.

To elucidate these rotational diffusion phenomena a great effort has been made by many investigators, and many theoretical treatments have been proposed, of which Einstein's equation (2) is the generally accepted one. In Einstein's equation, the rotational diffusion constant (Θ), the thermal energy (kT), and the rotational frictional coefficient (ζ) of the macromolecule are formulated as follows:

$$\Theta = \frac{kT}{\zeta} \qquad (1\text{-}1)$$

This is the fundamental equation relating the size and shape of the macromolecule to the measurable quantity, Θ.

The theoretical formulae for ζ in relation to the major dimensions of model anisometric macromolecules are given by Perrin (3) and Gans(4) for ellipsoids of revolution, and Burgers (5) and Broersma (6) for rod. Thus, the measurment of rotational diffusion constant can lead to the determination of the dimension of the macromolecule. The final equations available for calculating the dimensions from the rotational diffusion constant are:

for prolate ellipsoid of revolution (a>5b) **(Perrin)**

$$\Theta_p = \frac{3kT}{16\pi\eta_s a^3}\left[2\ln\frac{2a}{b} - 1\right] \qquad (1\text{-}2)$$

for oblate ellipsoid of revolution (b>5a) (Perrin)

$$\Theta_o = \frac{3kT}{32\eta_s b^3} \qquad (1\text{-}3)$$

for rod (closed cylinder) (a>5b) (Burgers)

$$\Theta_r = \frac{3kT}{8\pi\eta_s a^3}\left[\ln\frac{2a}{b} - 0.8\right] \qquad (1\text{-}4)$$

where η_s is the viscosity of the medium at temperature T, k is the Boltzmann's constant, and a and b are the lengths of the revolutional and the equatorial semi-axes of the model, respectively.

Among the methods which have been proposed to measure the rotational diffusion constants of anisometric macromolecules, there is the utilization of orientation birefringence. There are, however, many ways in which orientation birefringence can be determined and these are compared in Table I.

The streaming and the electric birefringence methods have been used more frequently, whereas the magnetic birefringence has rarely been measured. In the streaming birefringence method, the shearing stress of a streaming medium is applied as the force and this hydrodynamic interaction leads to the orientation of the suspended macromolecules. An additional measurable quantity is the optical anisotropy factor which is closely related to the optical polarizabilites of macromolecules. In the electric birefringence method, an electric field is applied, and the electric interaction preserves the orientation of the macromolecules. There is only one method, the saturating electric birefringence method, which is capable of determining the additional quantities, the optical anisotropy factor and the electrical polarizabili-

ties of the macromolecule. However, the saturating electric birefringence technique is difficult to handle, and the ordinary electric birefringence method cannot evaluate the parameters of interest.

The electric-streaming birefringence method is originally proposed as a method using two externally applied forces simultaneously. It would be of great interest to know how the macromolecules behave under the influence of two external forces which have different kinds of interaction, i.e., hydrodynamic and electric.

The mechanical structure of the streaming birefringence apparatus of the concentric cylinder type (Couette type) in which two metal cylinders are used, seemed to the author a good starting point for the development of an electric-streaming birefringence apparatus. Since the width of the annular gap is designed to be sufficiently small in comparison with the mean radius of the annular gap, it seemed possible that the concentric cylinders could be used as parallel plate electrodes. In this situation the directions of the two external fields are perpendicular to each other, that is, the hydrodynamic one is tangential and the electric one is radial to the concentric cylinders.

It can be imagined that when the annular gap is filled with a dilute solution of anisometric macromolecules and the apparatus is made ready to measure the streaming birefringence without rotation of the cylinder, if an electric potential gradient is applied between the two cylinders, the solution will become birefringent and a sensitive measurement of the extinction angle can be made at the 0, $\pi/2$, π, and $3\pi/2$ positions of the annular gap with respect to the axis of the polarizer (or analyzer), since the mean direction of the orientating macromolecular axis will, in most cases, be coinci-

dent with the electric field. Now, if one of the cylinders is made to rotate in the manner of the streaming birefringence method, in addition to the applied electric field, the magnitude of birefringence will again change, and the extinction angle will therefore deviate from the original value, and the extent of this deviation will depend upon the strength of hydrodynamic interaction. The magnitude of birefringence and the extinction angle in this situation may be evaluated by competition (or coordination) of the two external forces. In the case of competing orientation there will be an equilibrium between the two forces with respect to the axial orientation, which may be manufasted by the extinction angle at $\pi/4$. Moreover, when the strength of the electric interaction becomes small in comparison to the hydrodynamic one, both the magnitude of birefringence and the extinction angle will approach the values expected in streaming birefringence only.

The experimental definition of extinction angle in the electric-streaming birefringence method should, then, be changed from that of the streaming birefringence to "the extinction angle of electric-streaming birefringence is an angle in the region from $\pi/2$ to 0, the sense of decreasing angle being similar to that of streaming birefringence."

The theoretical behavior of macromolecular orientation under the influence of two external forces is expected to be explained by an analogous treatment to streaming birefringence based on the diffusion equation,

$$\frac{\partial f}{\partial t} = \textcircled{H}\nabla^2 f - div\, f\omega \qquad (1\text{-}5)$$

and the optical theory of orientation birefringence. In Eq. (1-5), f is the distribution function, and ω is the angular velocity of the macromolecules in the external fields.

The electrical properties of macromolecules will be determined by the theory of electric-streaming birefringence and the optical anisotropy factor can be determined by the theory of streaming birefringence (which is the special case of electric-streaming birefringence where the electric field stength = 0.)

On the other hand, the electric-streaming birefringence can also be carried out with an alternating electric field (as was done by O'Konski and Haltner (8) in their experiments on birefringence). It can be imagined that under the influence of a hydrodynamic and an alternating electric field the magnitude of birefringence will change, as shown in electric birefringence experiments, with applied frequency and voltage and there will be an additional steady birefringence caused by the streaming. This should be a more sensitive and simple way to distinguish the entities of electric interaction, that is, the permanent and induced dipole moments, in the extinction angle measurement, since extinction angle measurements are usually carried out in the time-average position of the cross of isocline. In the case of permanent dipole orientation, the extinction angle will be observed to move at very low frequency of applied electric field and with increasing frequency (at the constant voltage) it will be observed as apparently stationary. At very high frequency values, the value of extinction angle will be smaller than that expected from the effective voltage (Vrms), because of the decreasing possibility of macromolecular rotation following the alteration of the

applied electric field and a sort of orientation dispersion much like dielectric dispersion will result. In the case of induced dipole orientation, these phenomena will not occur because of the ability to follow the alternating electric field. At some very high frequency, a dispersion phenomena will occur because of the retardation of induced dipole formation.

Hence, the extinction angle measurement in an alternating electric field together with a hydrodynamic field will be a new way to estimate the individual dipole moment.

IN THE PRESENT ARTICLE the electric-streaming birefringence method is proposed for the simultaneous investigation of the rotational diffusion constant and the electrical and optical properties of macromolecules. The apparatus developed is a modification of the usual one for streaming birefringence so as to permit the application of an electric field together with a hydrodynamic field. The results so obtained are compared with the theory of electric-streaming birefringence. Some results of the electric-streaming birefringence technique when used with an alternating electric field (that is, orientation dispersion) are also presented.

Table 1 Methods of Orientation Birefringence

Birefringence	Orientation External Force	Measurable Quantities in addition to the Rotational Diffusion Constant
Streaming B. (Maxwell Effect)	Velocity Gradient	Optical Anisotropy Factor
Electric B. (Kerr Effect)	Electric Field	Electric Moment Optical Anisotropy Factor
Magnetic B. (Cotton-Mouton E.)	Magnetic Field	Magnetic Moment
Acoustic B.	Pressure Gradient	
Electric-streaming B.	Velocity Gradient Electric Field	Electric Moment Optical Anisotropy Factor

II. Theory

IIa Two Dimensional Expression of Electric-streaming Birefringence

A preliminary treatment on the two dimensional motion of a model macromolecule can throw a light on the comparative study of three dimensional problems as shown by Boeder [9] in his study of streaming birefringence.

i) Motion of a thin rod model in electric and hydrodynamic fields

A very thin rod with no flexibility has an axis of revolution 2a and a (neglected) diameter 2b and is assumed as a model for a macromolecule suspended isolatedly in an insulating medium filled in the annular gap between concentric cylinder in the apparatus. It is further assumed that the rod is carrying a permanent dipole moment μ along the axis of revolution and principal electric polarizabilities g_e along each of the two geometrical axes of the rod. The values of these electrical parameters are represented as the same notations with suffix 1 or 2, which shows the direction of the vector parallel to the axis of revolution or perpendicular to it, respectively.

The model rod can be placed in the xy-plane of the fixed co-ordinate where the positive x-direction is taken to be the direction of the positive electric field and the positive y-direction to be coincident with the stream line, when fields are applied.

The angular position of the rod is expressed by an angle φ which is an angle between the x-axis and the axis of revolution of the rod. (Fig. 2-1)

When one of the concentric cylinders is driven with a constant angular velocity, the rod is forced to move by the velocity gradient (G) of the streaming medium translationally and rotationally. The rod rotates around the center of mass with an angular velocity

$$\omega_{\varphi(G)} = G\cos^2\varphi \qquad (2\text{-}1)$$

When an electric potential gradient is applied between two cylinders (from -x- to +x-direction), the model in the gap is affected by the electric field (E) to the extent of the interaction of the permanent dipole moment, (μ_1^*) and E. (The motion μ_1^* represent the strength of permanent dipole moment in the medium.) The rod will be rotated under the influence of the torque ($M_{\varphi(E,\mu)} = -\mu_1^* E\sin\varphi$) exerted by the interaction. Since the angular velocity is given by

$$\omega = \frac{M}{\zeta} \qquad (2\text{-}2)$$

where,
$$\zeta = \frac{kT}{\Theta} \qquad (1\text{-}1)$$

the angular velocity ($\omega_{\varphi(E,\mu)}$) resulting from the E-μ interaction is

$$\omega_{\varphi(E,\mu)} = -\frac{\Theta}{kT}\mu_1^* E\sin\varphi \qquad (2\text{-}3)$$

On applying an electric field, there will occur the induced electric moment $g_e E$ corresponding to the extent of E and that of electrical polarizabilities g_e of the rod. This sort of induced moment will behave like the permanent dipole moment and a torque $M_{\varphi(E,g_e)} = -(g_{e1}-g_{e2})E^2\sin\varphi\cos\varphi$ generated by the interaction can lead the rotation of the rod with an angular velocity

$$\omega_{\varphi(E,g_e)} = -\frac{\Theta}{kT}(g_{e1}-g_{e2})E^2\sin\varphi\cos\varphi \qquad (2\text{-}4)$$

Fig. 2-1 Two Dimensional Representation of Rod Model in Annular Gap

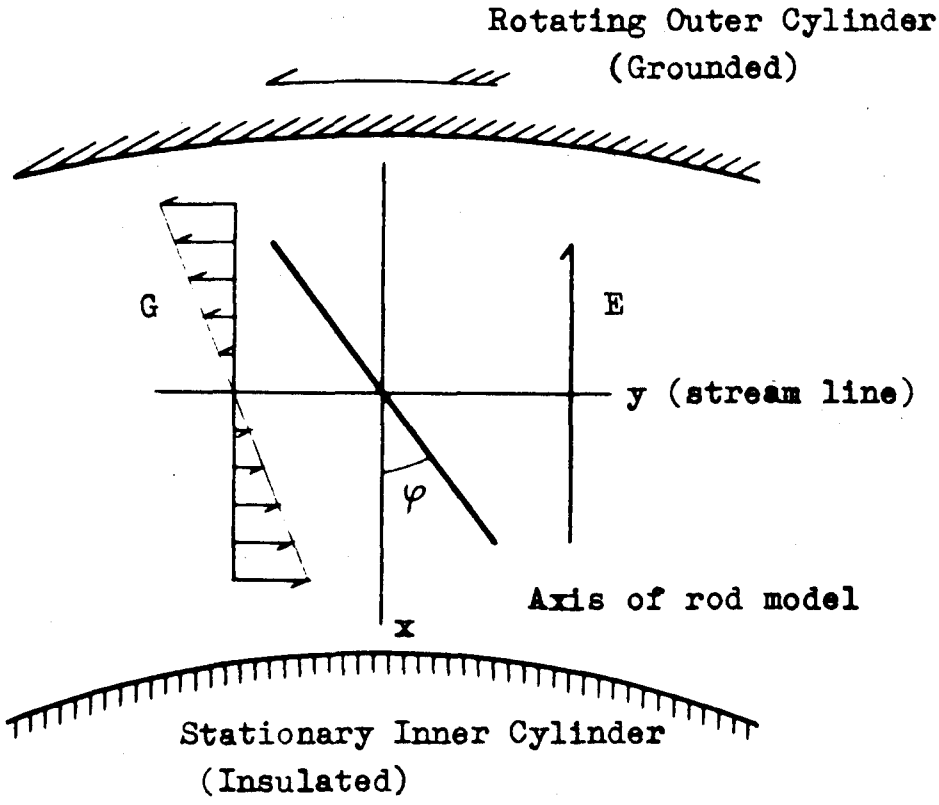

The total angular velocity ω_φ of the rod under the influence of two external forces of G and E will be given by adding three angular velocities shown in Eqs. (2-1), (2-3) and (2-4);

$$\omega_\varphi = \Theta \{ \alpha \cos^2\varphi - \beta \sin\varphi - \gamma^2 \sin\varphi \cos\varphi \} \tag{2-5}$$

where the notations

$$\begin{aligned} \alpha &= G/\Theta \\ \beta &= \mu_1^* E/kT \\ \gamma^2 &= (g_{e1} - g_{e2}) E^2/kT \end{aligned} \tag{2-6}$$

are used for simplification.

ii) Two dimensional distribution function

The two dimensional motion of a rod in a suspending medium under the influence of external forces will be expressed by the following diffusion equation, with a two dimensional distribution function of rod axis;

$$\frac{df(\varphi)}{dt} = \Theta \frac{d^2 f(\varphi)}{d\varphi^2} - \frac{d}{d\varphi}\left(f(\varphi) \cdot \omega_\varphi \right) \tag{2-7}$$

Inserting Eq. (2-5) into Eq. (2-7), one obtains

$$\frac{df(\varphi)}{dt} = \Theta \frac{d^2 f(\varphi)}{d\varphi^2} - \Theta \frac{d}{d\varphi} f(\varphi) \{ \alpha \cos^2\varphi - \beta \sin\varphi - \gamma^2 \sin\varphi \cos\varphi \} \tag{2-8}$$

At the steady state, the left term of Eq. (2-8) reduces to zero and a second order linear differential equation is obtained, that is,

$$\frac{d^2 f(\varphi)}{d\varphi^2} - \frac{df(\varphi)}{d\varphi}(\alpha \cos^2\varphi - \beta \sin\varphi - \gamma^2 \sin\varphi\cos\varphi) - f(\varphi)(\alpha \sin 2\varphi + \beta \cos\varphi + \gamma^2 \cos 2\varphi) = 0 \tag{2-9}$$

Eq. (2-9) cannot be solved by integration but with an assumption that all the values of parameters α, β, and γ^2 be much smaller than unity, it can be solved by means of expansion of $f(\varphi)$ to a power series. The solution may be put in the form

$$f(\varphi) = \sum_{\lambda=0}^{\infty} \sum_{\mu=0}^{\infty} \sum_{\nu=0}^{\infty} \alpha^\lambda \beta^\mu \gamma^{2\nu} \cdot f_{\lambda\mu 2\nu} \tag{2-10}$$

where $f_{000} = 1$.

Then, one can obtain $f_{\lambda\mu\nu}$ as follows:

$$
\begin{aligned}
f_{100} &= \frac{1}{4}\sin 2\varphi \\
f_{010} &= \cos\varphi \\
f_{200} &= -\frac{1}{64}\cos 4\varphi - \frac{1}{16}\cos 2\varphi \\
f_{110} &= \frac{1}{8}\sin 3\varphi + \frac{5}{8}\sin\varphi \\
f_{020} &= \frac{1}{4}\cos 2\varphi \\
f_{002} &= \frac{1}{4}\cos 2\varphi \\
f_{300} &= -\frac{1}{64}\left(\frac{1}{24}\sin 6\varphi + \frac{3}{8}\sin 4\varphi + \frac{9}{8}\sin 2\varphi\right) \\
f_{210} &= -\frac{1}{128}\left(\frac{24}{25}\cos 5\varphi + \frac{73}{9}\cos 3\varphi + 61\cos\varphi\right) \\
f_{120} &= f_{102} = \frac{1}{32}\sin 4\varphi + \frac{1}{16}\sin 2\varphi \\
f_{030} &= \frac{1}{24}\cos 3\varphi - \frac{1}{8}\cos\varphi \\
f_{012} &= \frac{1}{8}\cos 3\varphi + \frac{1}{8}\cos\varphi
\end{aligned}
\qquad (2-11)
$$

= = = = = = = = = = = = = = =

The final solution one thus approaches is

$$
\begin{aligned}
f(\varphi) = 1 &+ \frac{\alpha}{4}\sin 2\varphi + \beta\cos\varphi - \frac{\alpha^2}{64}(\cos 4\varphi + 4\cos 2\varphi) + \frac{\alpha\beta}{8}(\sin 3\varphi + 5\sin\varphi) \\
&+ \frac{(\beta^2+\gamma^2)}{4}\cos 2\varphi - \frac{\alpha^3}{64}\left(\frac{1}{24}\sin 6\varphi + \frac{3}{8}\sin 4\varphi + \frac{9}{8}\sin 2\varphi\right) \\
&- \frac{\alpha^2\beta}{128}\left(\frac{24}{25}\cos 5\varphi + \frac{73}{9}\cos 3\varphi + 61\cos\varphi\right) + \frac{\alpha(\beta^2+\gamma^2)}{32}(\sin 4\varphi + 2\sin 2\varphi) \\
&+ \frac{\beta^3}{24}(\cos 3\varphi - 3\cos\varphi) + \frac{\beta\gamma^2}{8}(\cos 3\varphi + \cos\varphi) + \cdots\cdots
\end{aligned}
\qquad (2-12)
$$

iii) Extinction angle in two dimensional orientation

According to the Boeder's treatment[9], the extinctiom angle which may be measurable in the two dimensional experiment of orientation birefringence is given by the following equations.

$$
-\cot 2\chi = \frac{A}{B} \qquad (2-13)
$$

where

$$A = \int_0^{2\pi} f(\varphi) \cos 2\varphi \, d\varphi \qquad (2\text{-}14)$$

$$B = \int_0^{2\pi} f(\varphi) \sin 2\varphi \, d\varphi$$

A and B are obtained from the distribution function to be:

$$A = -\frac{\pi}{16}\alpha^2 + \frac{\pi}{4}(\beta^2+\gamma^2) + \cdots \qquad (2\text{-}15)$$

$$B = \frac{\pi}{4}\alpha - \frac{\pi}{64}\frac{9}{8}\alpha^3 - \frac{\pi}{16}\alpha(\beta^2+\gamma^2) + \cdots$$

and we obtain

$$-\cot 2\chi = \frac{-\frac{1}{4}\alpha^2 + \frac{1}{4}(\beta^2+\gamma^2) + \cdots}{\alpha - \frac{9}{32}\alpha^3 - \alpha(\beta^2+\gamma^2) + \cdots} \qquad (2\text{-}16)$$

Neglecting the higher terms in Eq. (2-16)

$$\cot 2\chi = \frac{\alpha}{4} - \frac{(\beta^2+\gamma^2)}{\alpha} \qquad (2\text{-}17)$$

or

$$\cot 2\chi = \frac{G}{4\Theta} - \frac{\Theta}{G}\left(\frac{\mu_a E}{kT}\right)^2$$

where

$$\mu_a^2 = \mu_1^{*2} + (g_{e1} - g_{e2})kT \qquad (2\text{-}18)$$

IIb Theory of electric-streaming birefringence

i) Motion of an ellipsoidal model under the influence of both hydrodynamic and electric fields

In the generalized treatment on three dimensional theory, the model is taken to be a rigid ellipsoid of revolution with a length of revolutional axis 2a and an equatorial diameter 2b. The model ellipsoid has a permanent dipole moment u along the revolutional axis which takes an apparent moment μ_1^* in dielectric medium. (cf. IIa, i) The principal axes of electrical polarizabilities g_e are assumed to be coincident with the geometrical

axes of ellipsoid of revolution and the principal values of electrical polarizabilities are g_{e1} along the revolutional axis and g_{e2} along the direction perpendicular to it.

By the direction of the revolutional axis of the ellipsoid, the angular position of the model can be designated in a polar coordinate (θ, φ) with respect to the fixed rectangular coordinate (x, y, z), in which x is the direction of the cylinder radius (and alos of electric field), y is the tangential direction of cylinder (and also of laminar stream), z is the direction of polarized transmitting light. (cf. Fig. 2-2)

The ellipsoid is exerted by a shearing stress of laminar stream

$$\bar{u} = (0, G_x, 0)$$

and by an electric field

$$\bar{E} = (E, 0, 0)$$

The ellipsoid rotates in the natural manner (rotational Brownian movement) and is also forced to rotate by these two forces.

According to Jeffery[10], the angular velocity of an ellipsoid in laminar stream is given by

$$\omega_{\theta(G)} = \frac{R}{4} G \sin 2\theta \sin 2\varphi$$
$$\omega_{\varphi(G)} = \frac{1}{2} G (1 + R \cos 2\varphi) \qquad (2\text{-}19)$$

where $R = (a^2 - b^2)/(a^2 + b^2)$ (for prolate $R>0$, and for oblate $R<0$)

The torque exerted on the permanent dipolar ellipsoid in an electric filed is calculated as

$$M_{\theta(E,\mu)} = \mu_1^* E \cos\theta \cos\varphi$$
$$M_{\varphi(E,\mu)} = -\mu_1^* E \sin\varphi \qquad (2\text{-}20)$$

The relation of torque with the angular velocity of rotation of ellipsoid is given in the similar form as Eq. (2-2), so that the angular velocity with which the ellipsoid is rotated is given as;

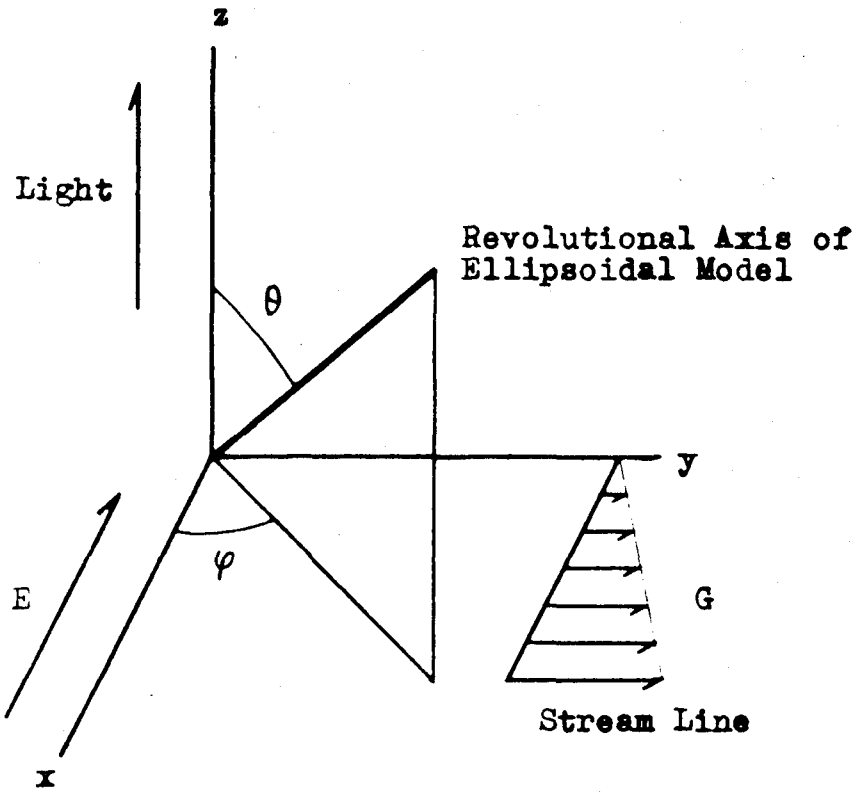

Fig. 2-2 Representation of the Revolutional Axis of Ellipsoidal Model in the Polar Coordinate

$$\omega_{\theta(E,\mu)} = \frac{\mu_i^* E}{kT} \Theta \cos\theta \cos\varphi$$
$$\omega_{\varphi(E,\mu)} = -\frac{\mu_i^* E}{kT} \Theta \frac{\sin\varphi}{\sin\theta} \qquad (2\text{-}21)$$

The electrical polarizabilities of the ellipsoid are affected by the applied field. By the interaction of electrical polarizabilities with the applied electric field, an electric moment, so called 'an induced dipole moment' is generated in the ellipsoid. By the simultaneous interaction of the induced dipole moment with the electric field, the torque exerted on an ellipsoid. The extent of torque and the corresponding angular velocity with which the ellipsoid is rotated can be calculated in the similar manner with permanent dipole interaction, that is,

$$M_{\theta(E,\gamma_e)} = (\gamma_{e1} - \gamma_{e2}) E^2 \sin\theta \cos\theta \cos^2\varphi$$
$$M_{\varphi(E,\gamma_e)} = -(\gamma_{e1} - \gamma_{e2}) E^2 \sin\theta \sin\varphi \cos\varphi \qquad (2\text{-}22)$$

and,

$$\omega_{\theta(E,\gamma_e)} = \frac{(\gamma_{e1} - \gamma_{e2})}{kT} E^2 \Theta \sin\theta \cos\theta \cos^2\varphi$$
$$\omega_{\varphi(E,\gamma_e)} = \frac{-(\gamma_{e1} - \gamma_{e2})}{kT} E^2 \Theta \sin\varphi \cos\varphi \qquad (2\text{-}23)$$

The total angular velocity is, then, given by adding all three angular velocities.

$$\omega_\theta = \Theta\left\{\frac{\alpha}{4} R \sin 2\theta \sin 2\varphi + \beta \cos\theta \cos\varphi + \gamma^2 \sin\theta \cos\theta \cos^2\varphi\right\}$$
$$\omega_\varphi = \Theta\left\{\frac{\alpha}{2}(1 + R\cos 2\varphi) - \beta \frac{\sin\varphi}{\sin\theta} - \gamma^2 \sin\varphi \cos\varphi\right\} \qquad (2\text{-}24)$$

where the notations α, β and γ^2 are the same as described in Eq. (2-6).

ii) Distribution function

Ellipsoidal macromolecule in a medium undergoes the Brownian movement and the rotational movement in which the angular velocity is represented by Eq. (2-24). The orientation of the principal axes of ellipsoids is distributed in the manner as given by a distribution function f, with which

the diffusion equation of axis of ellipsoid is given as

$$\frac{\partial f}{\partial t} = \Theta \nabla^2 f - \mathrm{div}\, f \cdot \omega \tag{1-5}$$

When the system reaches this steady state the left hand term of Eq. (1-5) reduces to zero. This, in the steady state, the distribution function f satisfies the following differential equation,

$$\Theta \left\{ \frac{1}{\sin\theta} \frac{\partial}{\partial\theta}\left(\sin\theta \frac{\partial f}{\partial\theta}\right) + \frac{1}{\sin^2\theta}\frac{\partial^2 f}{\partial\varphi^2} \right\} = \frac{1}{\sin\theta}\frac{\partial}{\partial\theta}(\sin\theta \cdot f\omega_\theta) + \frac{1}{\sin\theta}\frac{\partial}{\partial\varphi}(f\omega_\varphi \sin\theta) \tag{2-25}$$

Substituting Eqs. (2-24) into Eq. (2-25), one obtains

$$\begin{aligned} &\frac{\partial^2 f}{\partial\theta^2} + \cot\theta\frac{\partial f}{\partial\theta} + \frac{1}{\sin^2\theta}\frac{\partial^2 f}{\partial\varphi^2} \\ &= \alpha\left\{\frac{R}{4}\sin 2\theta \sin 2\varphi \frac{\partial f}{\partial\theta} + \frac{1+R\cos 2\varphi}{2}\frac{\partial f}{\partial\varphi} - \frac{3}{2}R\sin^2\theta \sin 2\varphi f\right\} \\ &+ \beta\left\{\cos\theta\cos\varphi\frac{\partial f}{\partial\theta} - \frac{\sin\varphi}{\sin\theta}\frac{\partial f}{\partial\varphi} - 2\sin\theta\cos\varphi f\right\} \\ &+ \gamma^2\left\{\sin\theta\cos\theta\cos^2\varphi\frac{\partial f}{\partial\theta} - \sin\theta\cos\varphi\frac{\partial f}{\partial\varphi} + (1+3\sin^2\theta\cos^2\varphi)f\right\} \end{aligned} \tag{2-26}$$

In order to solve Eq. (2-26), it is assumed that the velocity gradient of streaming medium and the strength of electric field are so small that α, β and γ^2 are much smaller than unity. Then, one may put the solution of the differential equation in the form as follows:

$$f = \sum_{\lambda=0}^{\infty}\sum_{\mu=0}^{\infty}\sum_{\nu=0}^{\infty} \alpha^\lambda \beta^\mu \gamma^{2\nu} \cdot f_{\lambda\mu 2\nu} \tag{2-27}$$

Here,

$$f_{000} = 1$$

Each term $f_{\lambda\mu 2\nu}$ can be expressed by a series expansion in terms of a spherical harmonics and then a series of differential equations can be solved successively. The final distribution function should satisfy the the normalization condition

$$\int_0^{2\pi}\int_0^{\pi} f \cdot \sin\theta \, d\theta \, d\varphi = 1 \tag{2-28}$$

so that the normalization constant being $1/4\pi$.

The distribution function of the axial orientation of the ellipsoid is then given by

$$f = \frac{1}{4\pi} \sum_{\lambda=0}^{\infty} \sum_{\mu=0}^{\infty} \sum_{\nu=0}^{\infty} \alpha^{\lambda} \beta^{\mu} \gamma^{2\nu} f_{\lambda\mu 2\nu} \qquad (2\text{-}29)$$

where

$$f_{000} = 1$$

$$f_{100} = \frac{R}{4} \sin^2\theta \sin 2\varphi$$

$$f_{010} = \sin\theta \cos\varphi$$

$$f_{200} = \frac{R}{16}\left\{R\left(-\frac{2}{15} + \frac{1}{4}\sin^4\theta\right) - \frac{2}{3}\sin^2\theta \cos 2\varphi - \frac{R}{4}\sin^4\theta \cos 4\varphi\right\}$$

$$f_{020} = f_{002} = \frac{1}{4}\left\{-\frac{2}{3} + \sin^2\theta + \sin^2\theta \cos 2\varphi\right\}$$

$$f_{110} = \frac{1}{8}\left\{(2\sin\theta + R\sin^3\theta)\sin\varphi + R\sin^3\theta \sin 3\varphi\right\}$$

$$f_{300} = \frac{R}{64}\left\{\left[-\left(\frac{4}{9} + \frac{2}{15}R^2\right)\sin^2\theta + \frac{1}{8}R^2\sin^6\theta\right]\sin 2\varphi - \frac{4}{15}R\sin^4\theta \sin 4\varphi - \frac{1}{24}R^2\sin^6\theta \sin 6\varphi\right\}$$

$$f_{030} = \frac{1}{24}\left\{(4\sin\theta - 3\sin^3\theta)\cos\varphi - \sin^3\theta \cos 3\varphi\right\}$$

$$f_{210} = \frac{1}{16}\left\{\left[\left(1 - \frac{2}{9}R + \frac{2}{15}R^2\right)\sin\theta - \frac{5}{36}R\sin^3\theta - \frac{1}{4}R^2\sin^5\theta\right]\cos\varphi + \left(\frac{25}{36}R\sin\theta + \frac{1}{8}R^2\sin^5\theta\right)\cos 3\varphi + \frac{1}{8}R^2\sin^5\theta \cos 5\varphi\right\}$$

$$f_{120} = f_{102} = \frac{1}{8}\left\{\left(\frac{1}{3} - \frac{1}{3}R + \frac{1}{2}R\sin^2\theta\right)\sin^2\theta \sin 2\varphi + \frac{1}{4}R\sin^4\theta \sin 4\varphi\right\} \qquad (2\text{-}30)$$

iii) Orientation birefringence

The modelized ellipsoidal macromolecule is assumed to have principal polarizabilities, the values of which are g_1 and g_2 along the revolutional and the transverse axis, respectively.

The optical theory of orientational birefringence had already been completed by Peterlin and Stuart, (11)

Since the electric-streaming birefringence is also a sort of orientation birefringence, , their theoretical results should be applied in this case. Following their theory, the optical theory of electric-streaming was treated with the given coordinates system described above and was found to yield identica results, as expected.

The final equations are:

$$-\cot 2\chi = \frac{A}{B} \tag{2-31}$$

$$\Delta n = \frac{2\pi\phi}{n}(g_1 - g_2)\sqrt{A^2 + B^2}$$

where

$$A = \int_0^{2\pi}\int_0^{\pi} f \sin^3\theta \cos 2\varphi \, d\theta \, d\varphi \tag{2-32}$$

$$B = \int_0^{2\pi}\int_0^{\pi} f \sin^3\theta \sin 2\varphi \, d\theta \, d\varphi \tag{2-33}$$

and $\chi = \pi/2 - \varphi$ the extinction angle, and $\Delta n = n_e - n_o$ the magnitide of birefringence, and ϕ is the volume fraction of ellipsoidal macromolecules in a solution, and n is the refraction index of solution.

By means of the expression of f in Eqs. (2-29) and (2-30), the integrals A and B are found to be

$$A = -\frac{R}{15}\left\{\frac{\alpha^2}{6} - \frac{\beta^2+\gamma^2}{R} + \cdots\cdots\right\}$$

$$B = \frac{R}{15}\left\{\alpha - \frac{1}{12}\left(\frac{1}{3} + \frac{R^2}{35}\right)\alpha^3 + \frac{1}{3}\left(\frac{1}{2} + \frac{R}{7}\right)\frac{\alpha(\beta^2+\gamma^2)}{R} + \cdots\right\} \tag{2-34}$$

(a) Extinction angle

The following equation can be obtained for the extinction angle of electric-streaming birefringence:

$$\cot 2\chi = \frac{\alpha}{6} - \frac{\beta^2+\gamma^2}{R\alpha} + \cdots\cdots$$

or

$$\cot 2\chi = \frac{G}{6\Theta} - \frac{\Theta}{RG}\left(\frac{\mu_a E}{kT}\right)^2 + \cdots\cdots \tag{2-35}$$

since $\beta^2 + \gamma^2 = (\mu_1^{*2} + (g_{e1} - g_{e2})kT)E^2/(kT)^2$ (2-6) cf.(2-18)

The graphic illustration is given in Fig. 2-3 of Eq. (2-35).

as the relation of the extinction angle χ with the parameter $\alpha = G/\Theta$ in which the quantity μ_a^2/R is used as a parameter and the absolute value of R is set to unity (corresponding with the largely anisometric ellipsoids of revolution).

In Fig. 2-3 it can be seen that: when μ_a^2/R is positive, the extinction angle decreases monotonously with increasing velocity gradient (α can be replaced by G since in the typical case, Θ should be constant over the given velocity gradient) from the initial value of 90° at $G = 0$. The initial slopes of decreasing χ can be calculated as

$$\left(\frac{\partial \chi}{\partial G}\right)_{\substack{E \neq 0 \\ G=0}} = -\frac{1}{2}\frac{R}{\mu_a^2}\frac{kT}{\Theta E^2} \qquad (2\text{-}36)$$

and at

$$G_{\chi=\frac{\pi}{4}} = \sqrt{\frac{6\mu_a^2}{R}}\frac{\Theta E}{kT} \qquad (2\text{-}37)$$

the extinction angle takes a value of 45°.

When μ_a^2/R is negative, the extinction angle increases with increasing G from the initial value of 0° at $G = 0$. The initial slopes of increasing χ can also be given by Eq. (2-36). After χ passes the maximum value

$$\chi_{max} = \frac{1}{2}\cot^{-1}\sqrt{-\frac{2\mu_a^2}{3R}}\frac{\Theta E}{kT} \qquad (2\text{-}38a)$$

at

$$G_{\chi=max} = \sqrt{-\frac{6\mu_a^2}{R}}\frac{\Theta E}{kT} \qquad (2\text{-}38b)$$

χ decreases monotonously to 0°.

It can be easily known from Eq. (2-35) that the cot 2χ-E^2 curves give the linear relation with an intercept $G/6\Theta$ and a slope

Fig. 2-3 Theoretical χ-G curves in Electric-streaming Birefringence

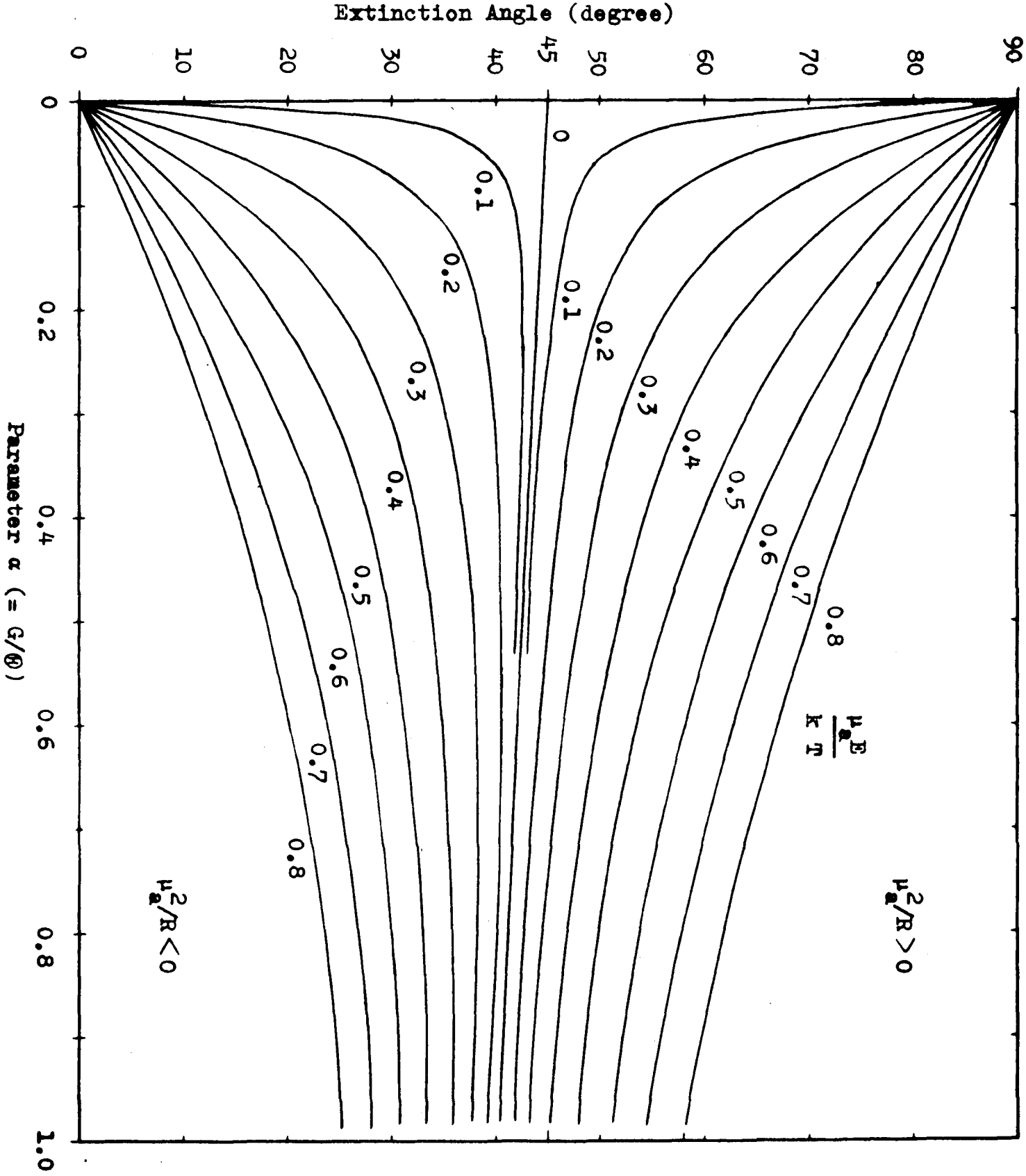

$$\left[\frac{\partial(\cot 2\chi)}{\partial(E^2)}\right]_{\substack{E=0\\G\neq 0}} = -\frac{\mu_a^2}{R}\frac{1}{G}\frac{\Phi}{kT} \tag{2-39}$$

(b) Magnitude of Birefringence

From Eqs. (2-32) and (2-34) one can obtain the equation for the magnitude of birefringence as follows:

$$\Delta n = \frac{2\pi\phi}{n}(g_1-g_2)\frac{R}{15}\left[\alpha^2 - \frac{1}{6}\left(\frac{1}{6}+\frac{R^2}{35}\right)\alpha^4 + \frac{2}{21}\alpha^2(\beta^2+\gamma^2) + \frac{1}{R^2}(\beta^2+\gamma^2)^2 + \cdots\right] \tag{2-40}$$

or

$$\Delta n = \frac{2\pi\phi}{n}(g_1-g_2)\frac{R}{15}\left[\left(\frac{G}{\Phi}\right)^2 - \frac{1}{6}\left(\frac{1}{6}+\frac{R^2}{35}\right)\left(\frac{G}{\Phi}\right)^4 + \frac{2}{21}\left(\frac{G}{\Phi}\right)^2\left(\frac{\mu_a E}{kT}\right)^2 + \frac{1}{R^2}\left(\frac{\mu_a E}{kT}\right)^4 + \cdots\right]$$

In Fig. 2-4 a graphic illustration of the theoretical equation (Eq. 2-40) is given in the case of R = 1. The ordinate is the orientation factor of electric-streaming birefringence.

The Δn-G curves show in the case of E = 0, $\Delta n = 0$ at G = 0 and the initial slope of the curve at E = 0 is

$$\left(\frac{\partial \Delta n}{\partial G}\right)_{\substack{E=0\\G=0}} = \frac{2\pi\phi}{n}(g_1-g_2)\frac{R}{15}\frac{1}{\Phi} \tag{2-41}$$

And in the case of $E \neq 0$, n at G = 0 is given by the equation of the electric birefringence, but the initial slope of the curve

$$\left(\frac{\partial \Delta n}{\partial G}\right)_{\substack{E\neq 0\\G=0}} = 0 \tag{2-42}$$

Fig. 2-4 Theoretical Curves of Electric-streaming Birefringence (R=1)

$$\Delta n \times \frac{15n}{2\pi\phi(g_1 - g_2)}$$

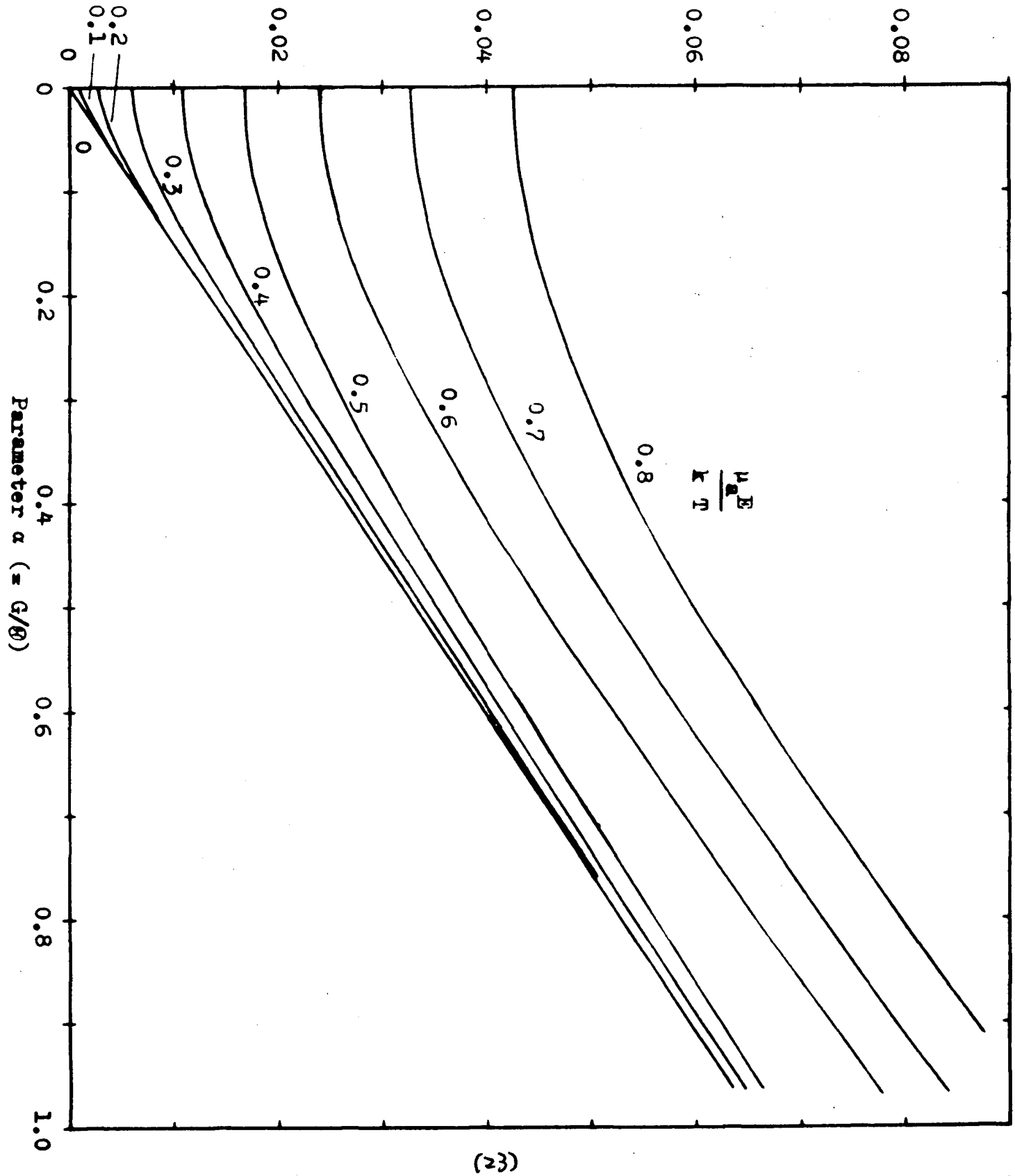

The sign of Δn is

$$(g_1-g_2)R > 0 \qquad \Delta n > 0, \quad (\partial \Delta n/\partial G) > 0$$

$$(g_1-g_2)R < 0 \qquad \Delta n < 0, \quad (\partial \Delta n/\partial G) < 0$$

The Δn-E^2 curves can be also derived, but these curves are variant depending on the optical anisotropy factor((g_1-g_2)), the shape (indicated by R) and the apparent electric parameter (μ_a).

In the case of no velocity gradient, G = 0, the usual Kerr effect (12) is derived. The slope of the line in the Δn-E^2 plot at G = 0 is

$$\left[\frac{\partial \Delta n}{\partial (E^2)}\right]_{\substack{E\neq 0 \\ G=0}} = \frac{2\pi\phi}{n}(g_1-g_2)\frac{R}{15}\left(\frac{\mu_a}{kT}\right)^2 \qquad (2\text{-}43)$$

And at $G \neq 0$, the curves have the initial slopes

$$\left[\frac{\partial \Delta n}{\partial (E^2)}\right]_{\substack{E=0 \\ G\neq 0}} = 0 \qquad (2\text{-}44)$$

III Method and Material

IIIa Experimental Method

The block diagram of the apparatus for the electric-streaming birefringence measurement is given in Fig. 3-1.

i) Apparatus

As the main equipment for the electric-streaming birefringence measurement, a concentric cylinder assembly for streaming birefringence, manufactured by Rao Instrument Company (Brooklyn, New York, U.S.A., model B-7, the mean diameter of the annular gap of 4.0 cm. with the gap width of 0.1 cm. and the depth of 10.2 cm.) was used with the modifications described below.

1. The stationary inner cylinder was insulated by inserting a polystyrene circle plate of 0.5 cm. thickness between the inner cylinder holder and the holder base of the main body. The cross-sectional sketch of the assembly is given in Fig. 3-2 in which dimensions are not drawn critically.

2. Accordingly, the rotary outer cylinder was made to slide up 0.5 cm. from its usual place, and was completely grounded electrically by means of a phosphorobronze brush shoe attached to be in contact with both a common grounded line and the rotatory cylinder.

3. The gum packing rings set between top and bottom windows and the outer cylinder were replaced by packing rings made from a Teflon sheet (Nippon Pillar Co.) to avoid the damage by some harmful solvents.

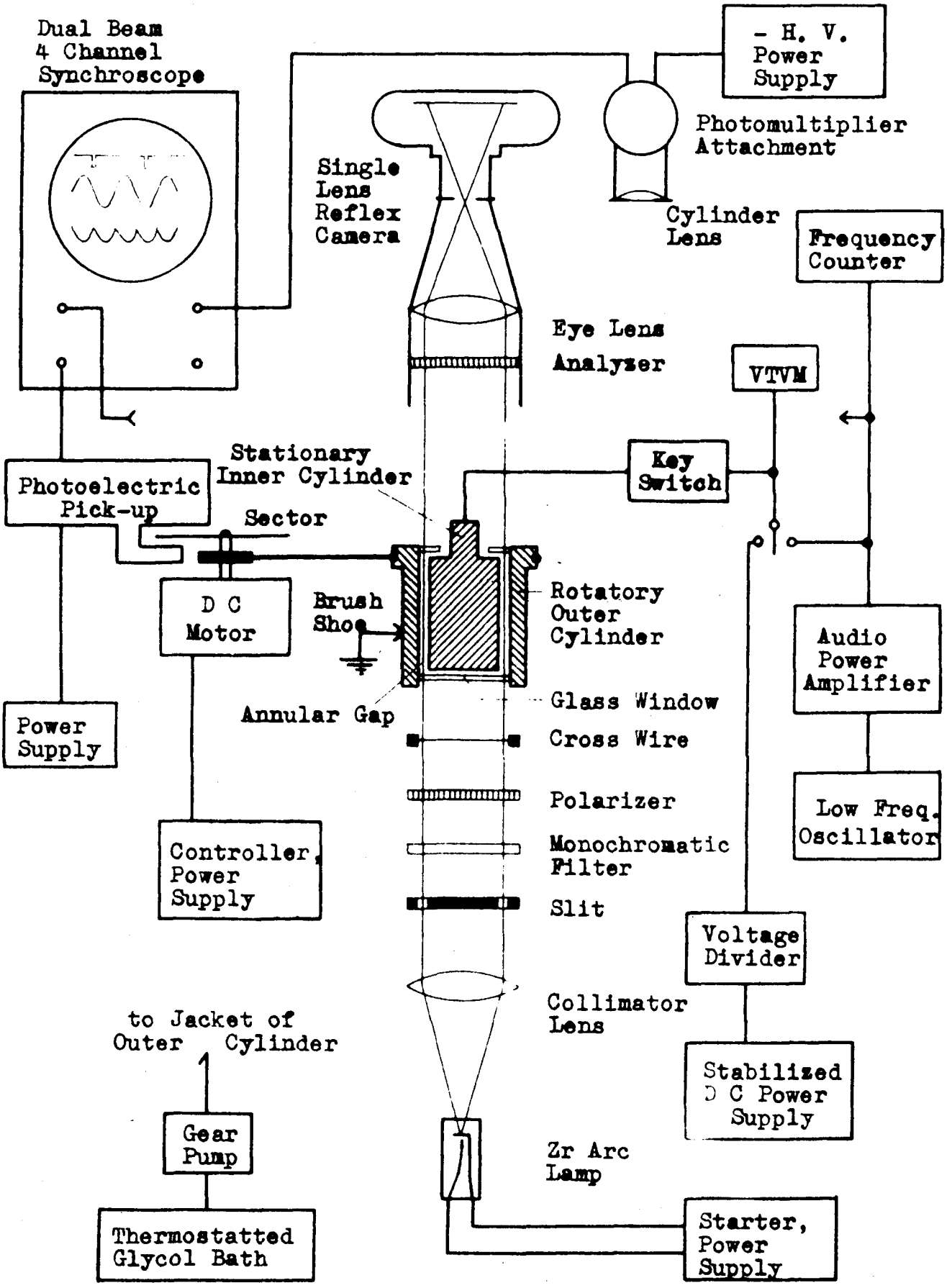

Fig. 3-1 Block Diagram of the Electric-streaming Birefringence Apparatus

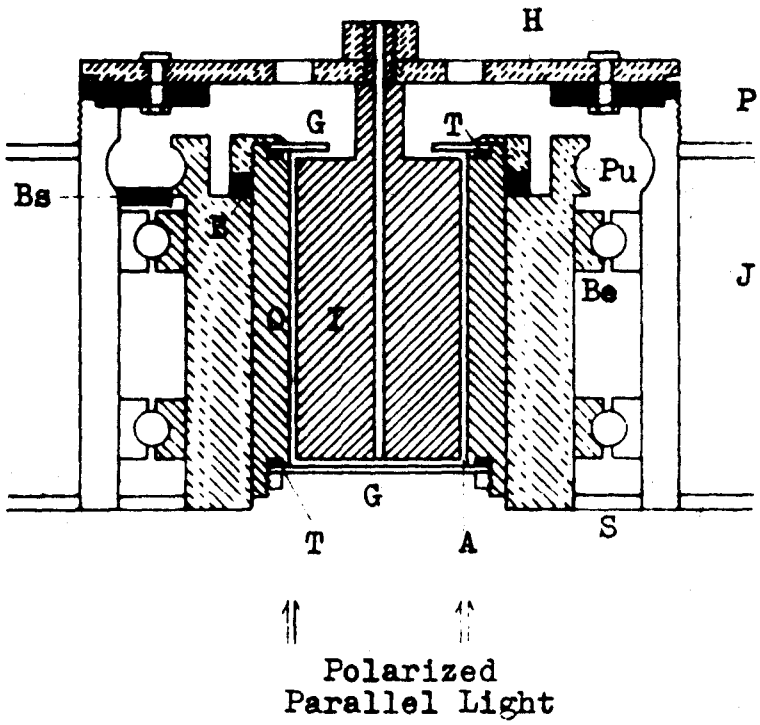

Fig.3-2 A Cross-sectional Sketch of Modified Cylinder Assembly

I: stationary inner cylinder, O: rotatory outer cylinder, G: glass window, H: inner cylinder holder, J: jacket, T: teflon ring packing, P: polystyrene plate, B: block to adjust the hight of outer cylinder, Bs: brush shoe, Be: bearing immersed in lubricating oil, S: seal, Pu: pulley for driving belt, A: annular gap.

4. The light source equipments, a Zirconium arc lamp and its starter, were replaced by components more readily available in Japan. (Ushio Industrial Co., type Z-25E and DSb-150).

5. In order to measure the extinction angle within a shorter time than by the usual method, a photographing method was employed. A single lens 35 mm. reflex camera (Asahi Optical Co., Asahiflex type B-II) was designed to be attached to the eye lens to catch the image of whole annular gap on the non-parallax finder (and also on the film).

6. The photographing attachment was movable and could be replaced by a photomultiplier attachment to measure the transmitting light intensity. The photomultiplier attachment was made by a cylindrical lens window and a photomultiplier (Toshiba MS-9S), to which a negative high voltage (-700 to -1200 V) was supplied from a common type voltage stabilizer.(13) The out-put voltage of the photomultiplier was introduced in one channel of the 4 channel dual beam synchroscope (Iwasaki Communications Apparatus Co., model DS-5155, 0-10 Mc, in-put impedence 10 MΩ).

Other optical arrangements, such as filters and a cross wire were used as in the original equipment. Also the driving DC motor and its power supply was from the original equipment. To compute the velocity gradient of streaming medium, an electro-optical pick-up was employed, for measuring the number of rotations of the motor. The pick-up was built up with a small light source and a phototransistor (Matsushita Electric Works, OCP-71). A sector was a circle plate from which a slit was cut off, and was placed on the pulley of the motor so as to be between the light source and the transistor. Thus, a signal appeared on the out-put of the pick-up every time the motor turned around to where light came to the transistor through a slit. The pulses were also introduced to the second channel of the synchroscope.

A stabilized DC voltage power supply of the usual type (250-400 V, 300 V 150 mA.)[13] was made for supplying the electrostatic field. A voltage divider was designed to be a simple resistance dividing circuit and connected to the line between the stabilizer and a key switch. A vacuum tube volt meter (VTVM) was employed to check the applied voltage. (Hansen Electronic Co., Model UV-47, in-put impedence 26 MΩ).

In the case of experiments with an alternating electric field, a low frequency oscillator (Kikusui Dempa, Model ORC-27) and an audio power amplifier (Sansui Electric Co., Model Q-55, 50 W) and a specially designed impedence matching transformer were arranged as a power source. The out-put voltage could be controlled up to 700 V p-p. by adjusting the out-put voltage of oscillator (in-put voltage of amplifier). The applied voltage was measured with VTVM and the applied frequency was computed with a frequency counter (Ono Instrument Co., Model FH-71, 0-1.2 Mc) and the wave form was observed by introducing the applied wave in the third channel of the synchroscope.

A key switch used for applying an electric potential on the stationary inner cylinder was the common"telegraph key" type. The normal position of the key was designed to be grounded to avoid charging of the condensor (the concentric cylinders).

Ethylene glycol was circulated from a temperature controlled glycol bath to the jacket of the concentric cylinder assembly to maintain the experimental temperature constant.

ii) Measurements

The optical system was adjusted by the usual method.[14] Also, the rotatory outer cylinder was driven by the usual method of belt driving.

The velocity gradient of streaming medium was calculated from the pulse interval of the photo-electric pick-up on the oscillograph.

The photographing method of extinction angle measurement was carried out by the following procedures.

1. The cross wire was set in the positions of 0, $\pi/2$, π, and $3\pi/2$ on the annular gap so as to indicate the axes of two polarizing filters, which were fixed to be perpendicular to each other regarding their polarizing planes.

2. The whole annular gap was photographed by the camera attachment described above on a tri-X class (ASA 200) 35 mm. film in each experiment.

3. The developed films had a common image, that is, a darkened circle (corresponding to a birefringent annular gap), four sharp transparent lines (arms of cross wire), and four transparent bands (arms of the cross of isocline), and a pair of transparent broad bands (arms of the inner cylinder holder) in the darkened circle. They were projected to be enlarged by a photo-enlarger (lens Hexanon 50 mm. f 1:3.5) on a circle protractor of 18 cm. in diameter. By adjusting the relative positions of the protractor and the negative film on the enlarger with the aid of images of the cross wire arms, the extinction angle was easily measured as an angle between one of the images of the cross wire arms and the center of the transparent image of the corresponding arm of the cross of the isocline. (As described above, the extinction angle was measured as an angle in one quadrant designated by the axes of the two polarizing filters and the sense of the decreasing angle was taken to be similar to that of streaming birefringence ($E = 0$, $G \neq 0$).

4. Four extinction angles were usually measured from one negative

film, so that they were averaged.

The measurement of transmitting light intensity was carried out with the photomultiplier attachment. The magnitude of intensity was measured as a deflection of oscillograph which was calibrated with angles of rotation of the analyzer from 90° position with regard to the polarizer. When the incident light was too intense to measure within the calibrated linear region of the oscillograph, a neutral filter (Kenko ND2 or ND4) was attached on the cylindrical lens window of the photomultiplier attachment to reduce the intensity.

The results of extinction angle and intensity measurements were corrected in the usual manner with the data obtained by reverse rotation of the outer cylinder in the identical condition.

IIIb Material

i) Poly-γ-benzyl-L-glutamate (PBLG)

Poly-γ-benzyl-L-glutamate used was a sample synthesized in dioxane with an initiator of sodium methoxide from N-carboxy-γ-benzyl-L-glutamate anhydride. The molecular weight of PBLG was determined from the intrinsic viscosity of dichloracetic acid solution with the molecular weight-intrinsic viscosity relation given by Doty, Bradbury, and Holzer.[15] It was found to be 206,000. This polymer was dissolved in a freshly distilled m-cresol for each experiments.

ii) Yellow bentonite

Yellow bentonite had been suspended in distilled water for one year. A 5 ml. of sample was taken from its supernatant and mixed with ethylene glycol (reagent grade) to a final volume of 100 ml. and served for each experiment.

IV EXPERIMENTAL RESULTS

IVa Electric-streaming Birefringence with Electrostatic Field (DC method)

i) Extinction angle of poly-γ-benzyl-L-glutamate.

A result obtained in the extinction angle measurements with an electrostatic and a hydrodynamic field are shown in Fig. 4-1. Measurements were carried out with a m-cresol solution of 0.243 w/v % at 21.0 ± 0.5° C.

The extinction angles at any given DC field started from 90° and decreased gradually and regularly with increasing velocity gradient. Then the sign of μ_a^2/R should be positive.

With the same PBLG solution of 0.127 w/v % the extinction angles were also measured in the identical condition and found to be in agreement with the values cited in Fig. 4-1.

From the initial slope of χ-G curve (Fig. 4-1, E = 0) the rotational diffusion constant was calculated to be 220 $sec.^{-1}$, which is in fair agreement with the value obtained with the electric birefringence measurement.(16)

In Fig. 4-2 the cot 2χ-E^2 relations are given which were obtained from replotting the result of Fig. 4-1.

The linear relation was obtained in the smaller DC field strength and, in common, the plots in the same velocity gradient had less value of cot 2χ with increasing DC field strength.

With the Eq. (2-39) the apparent electric parameter μ_a was calculated from the slopes of the lines in Fig. 4-2 and found to be 3200 D.

The cot 2χ-E^2 relation obtained from another solution (0.209%) and

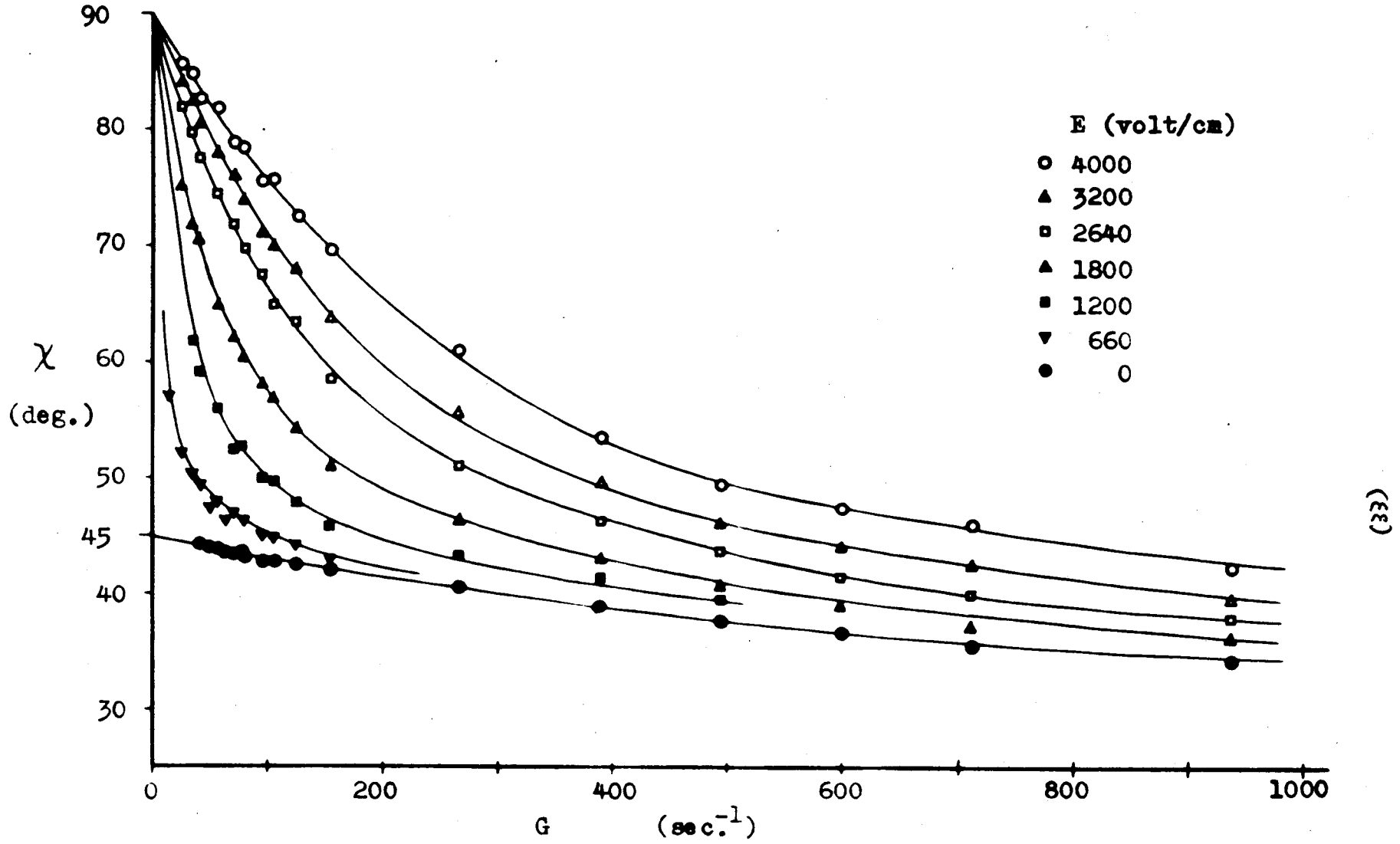

(33)

Fig. 4-1 Extinction Angle of PBLG (T-629) in m-cresol (0.243%) at 21.0°C

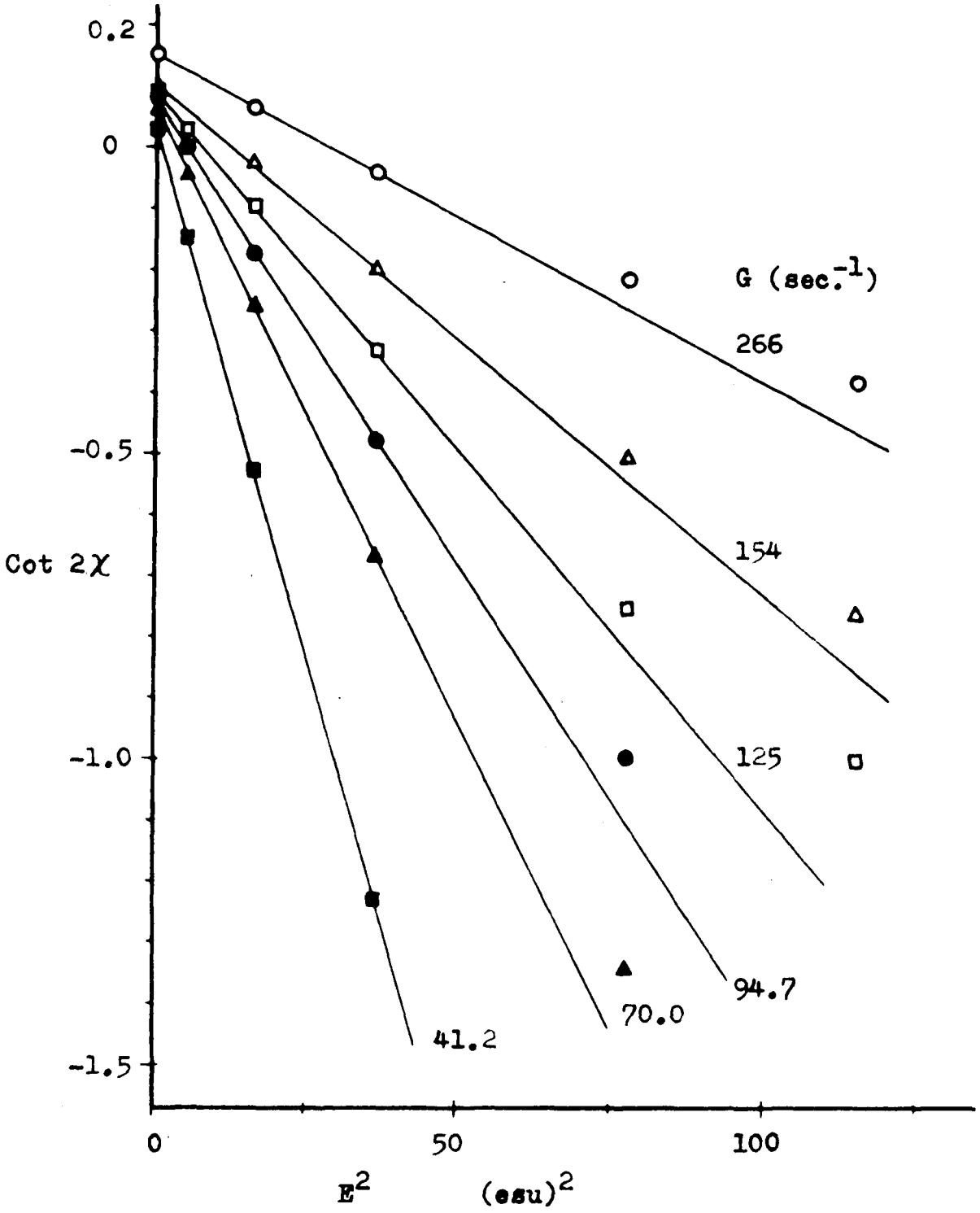

Fig. 4-2 Cot 2χ -E^2 Plot of Electric-streaming Birefringence with PBLG (T-629) in m-cresol

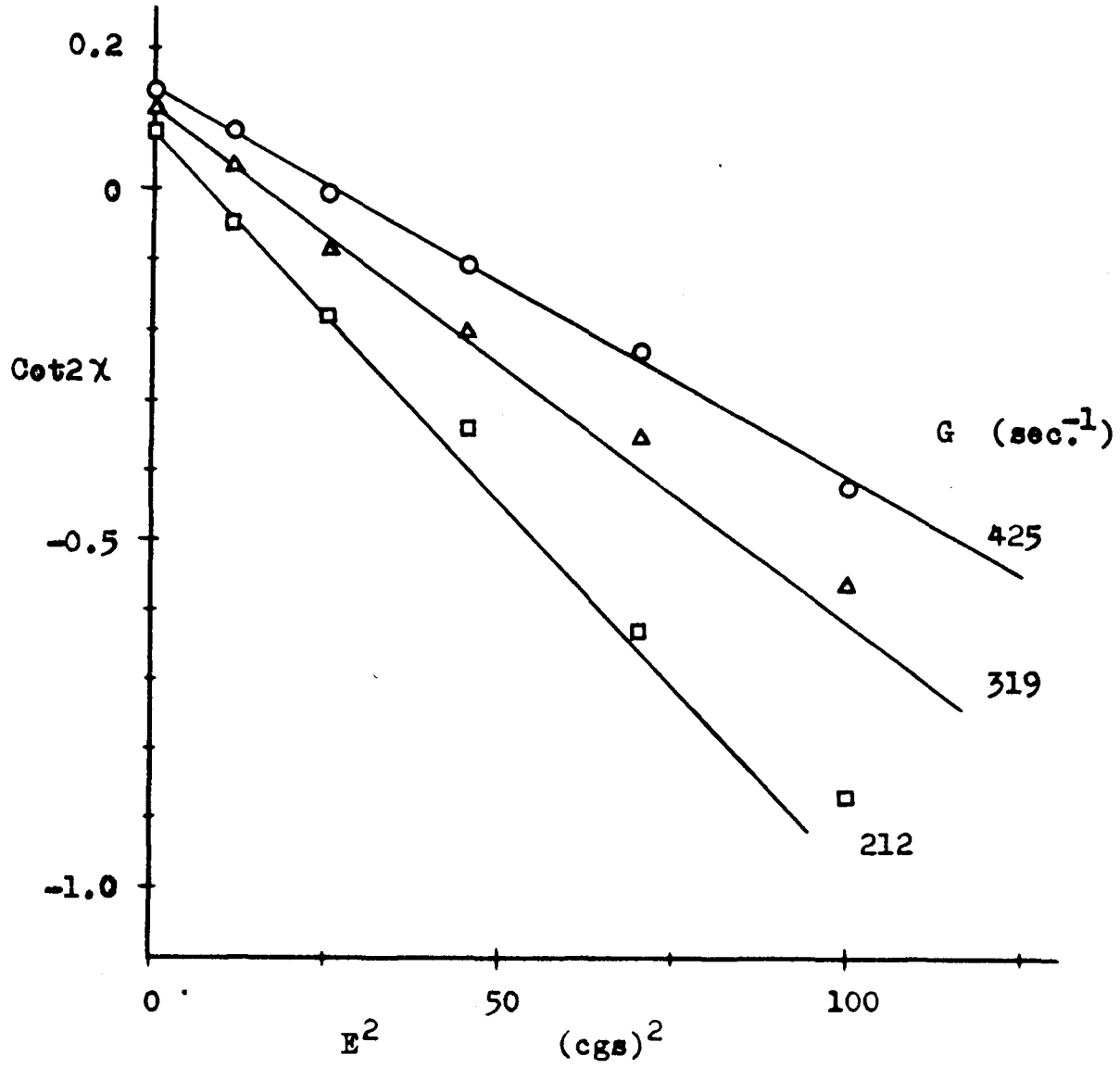

Fig. 4-3 Cot2χ -E^2 Plot of Electric-streaming Birefringence with PBLG in m-cresol (0.209%) at 31°C.

temperature (31.0 $\pm$ 1° C.) are given in Fig. 4-3. In this experiment the rotational diffusion constant was found to be 420 $sec.^{-1}$ and the apparent electric parameter as 3110 D.

ii) Transmitted light intensity of poly-γ-benzyl-L-glutamate.

In Fig. 4-4 the transmitted light intensity was plotted against the velocity gradient. Experiments were carried out at 21.0 $\pm$ 0.5° C with a solution of 0.243 w/v %.

The intensity was scaled arbitrarily on the ordinate, but each value was compared as described above.

In the smaller DC field strength the intensity increased with increasing velocity gradient in the manner expected from the theory, but in the higher DC field strength the results had the minimum value with increasing velocity gradient.

In both experiments of extinction angle and intensity some scattering of light was observed with increasing DC field strength. At larger velocity gradients the higher DC field strength was needed for the same amount of light scattering. The solution after repeated application of electric fields was tinged with orange-yellow.

iii) Extinction angle of yellow bentonite.

The χ-G plot and the cot 2χ-E^2 plot of yellow bentonite are shown in Fig. 4-5 (a) and (b), respectively. The experiments were carried out at 31 $\pm$ 1° C. The concentration of aqueous glycol suspension of yellow bentonite was determined by dry weight and found to be 0.033%.

The extinction angles decreased from 90° with increasing velocity gradient under the influence of electrostatic field. The sign of μ_a^2/R was found to be positive.

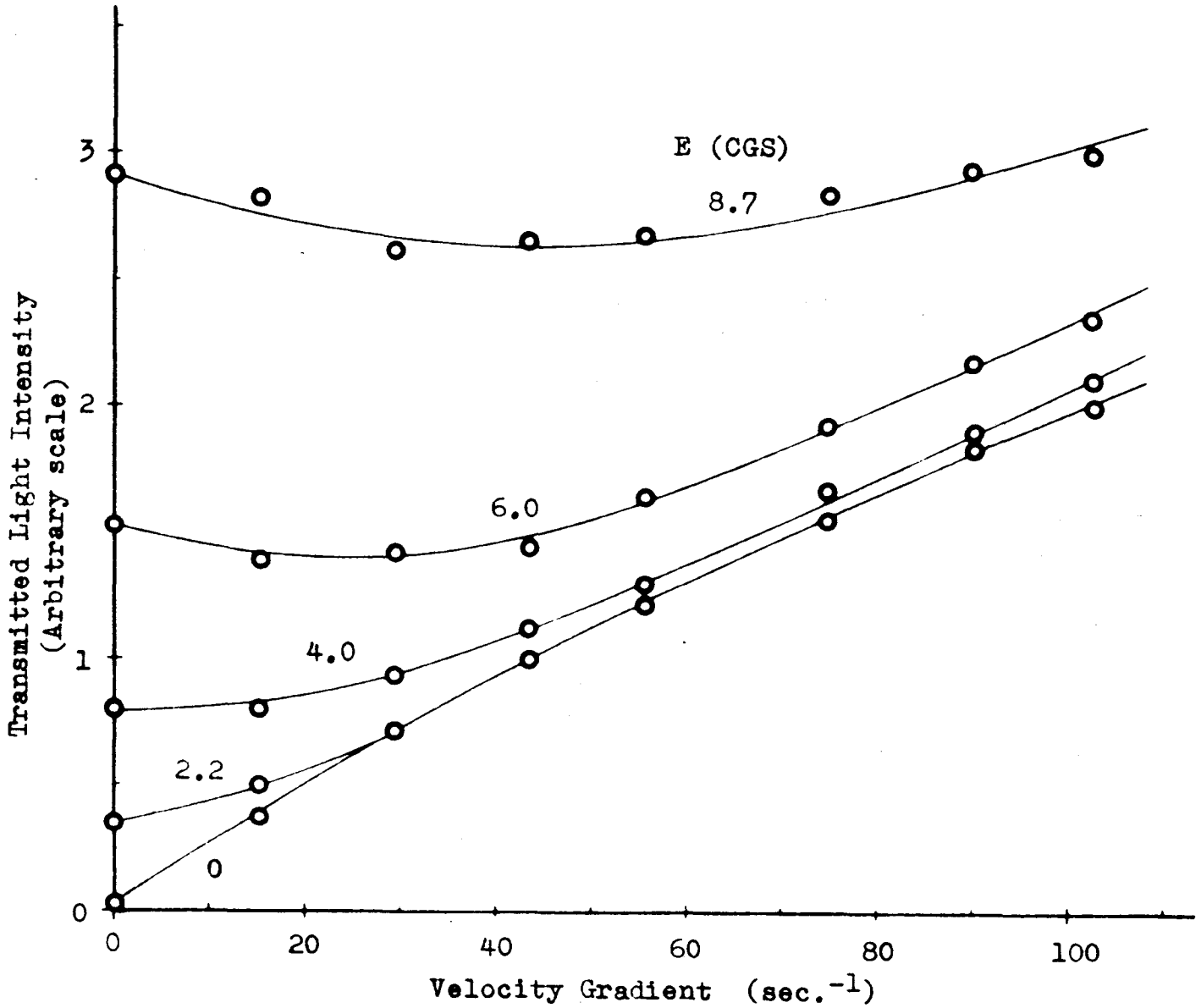

Fig. 4-4 Transmitting Light Intensity in Electric-streaming Birefringence with PBI : (T-629) in m-cresol

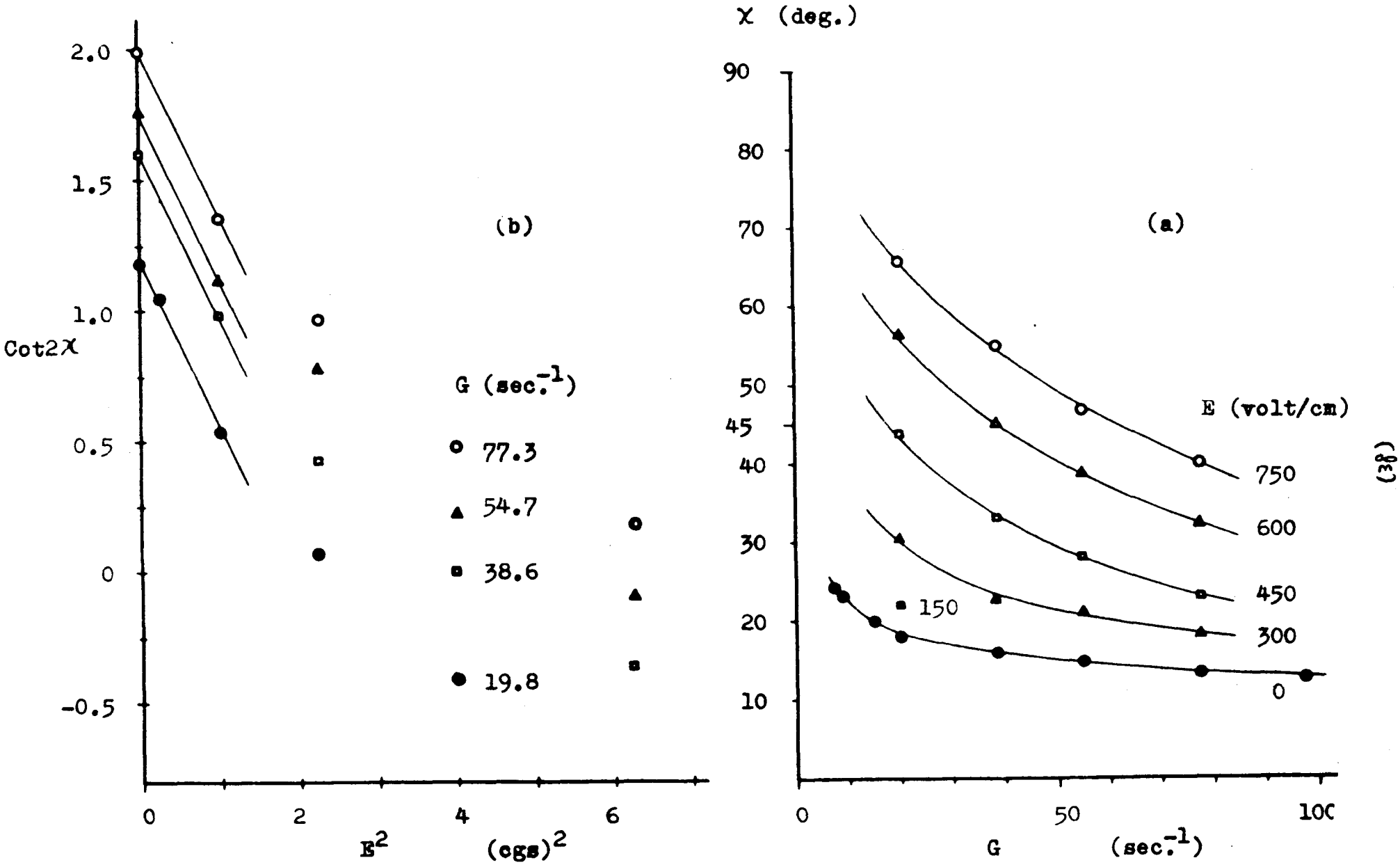

Fig. 4-5 χ-G Plot (a) and Cot2χ -E^2 Plot (b) of Electric-streaming Birefringence with Yellow Bentonite in 95% Aqueous Glycol (0.033%) at 31°C.

The χ-G curves showed the polydispersity of the sample and the rotational diffusion constant assumed from the angle by means of the numerical table varied from 1.5 to 3.3 $sec.^{-1}$ with increasing velocity gradient.

The cot 2χ-E^2 relation was not linear at any given velocity gradient and the initial slopes of the lines between the initial two points were found to be identical.

In the experiments of this aqueous glycol suspension of yellow bentonite, aggregation of suspensoid and, in the extreme case, small bubbles of gas were observed after long periods of application of the DC field.

IVb Electric-streaming Birefringence with Alternating Electric Field (AC method)

i) Extinction angle of poly-γ-benzyl-L-glutamate

The measurements of extinction angle with a hydrodynamic and an AC field were carried out at 31 $\pm$ 1° C with a 0.209 w/v % m-cresol solution of poly-γ-benzyl-L-glutamate. The results are given in Fig. 4-6.

The applied voltage was 300 Vrms (effective value) at all the frequencies in the experiment and for all velocity gradients. The sinusoidal waves of applied voltage included a slight amount of distortion in the applied frequencies below 70 c/s and over 3 kc/s.

The images of cross of isocline observed with the frequencies below 100 c/s were not so apparent. They appeared on applying an AC field and then diffused with time, so that the values plotted in Fig. 4-6 were taken from measurements repeated over ten times. These diffused images of cross of isocline were found to be apparent with increasing frequency and/or lowering the effective value of applied electric field. (In the latter case the values of the extinction angle were reduced.)

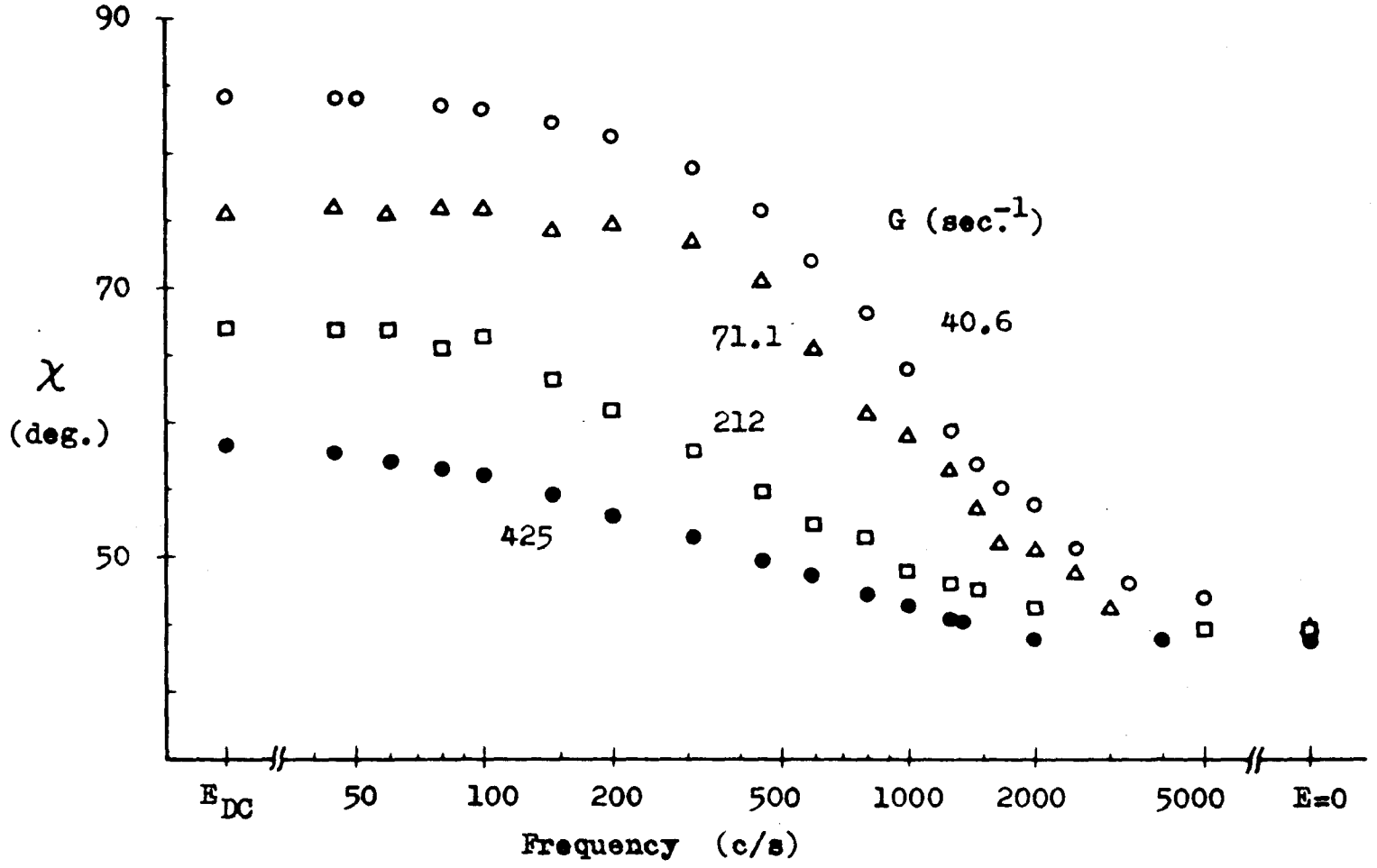

Fig. 4-6 Frequency Dependence of Extinction Angle in the Electric-streaming Birefringence of PBLG (T-629) in m-cresol under Constant E_{rms} (300V) and G (given in the figure).

Less darkness of cross of isocline was observed in this experiment as compared with that observed in the DC method.

The extinction angle measured at a given velocity gradient and an electric field strength (3000 Vrms/cm) changed with frequency. The extrapolation of values to zero frequency (DC) showed the identical value observed with an electrostatic field ($3000V_{DC}$/cm) in all experiments of a given velocity gradient, and the extrapolation to infinite frequency showed the identical value observed with each applied velocity gradient without electric field. Between these two extreme values the plots of extinction angle exhibited sigmoidal curves.

ii) Extinction angle of yellow bentonite.

In Fig. 4-7, results of electric-streaming birefringence under an alternating electric field and a hydrodynamic field are shown. The measurements were carried out at 31 $\pm$ 1° C with a 0.033 w/v % aqueous glycol (ca. 95 v/v %) suspension of yellow bentonite.

With bentonite it was found that the images of cross of isocline were apparent all over the applied frequency and the darkness of cross of isocline was not very different from that observed in the DC method. The suspension was more stable against the applied electric field as compared with the result of the DC method.

When the values were extrapolated to zero frequency they were coincident with those obtained in the DC method at the identical velocity gradient.

Within experimental error the extinction angle did not deviate within the frequency range examined in these experiments.

Other results obtained with different values of velocity gradient (not shown) showed the same characteristics.

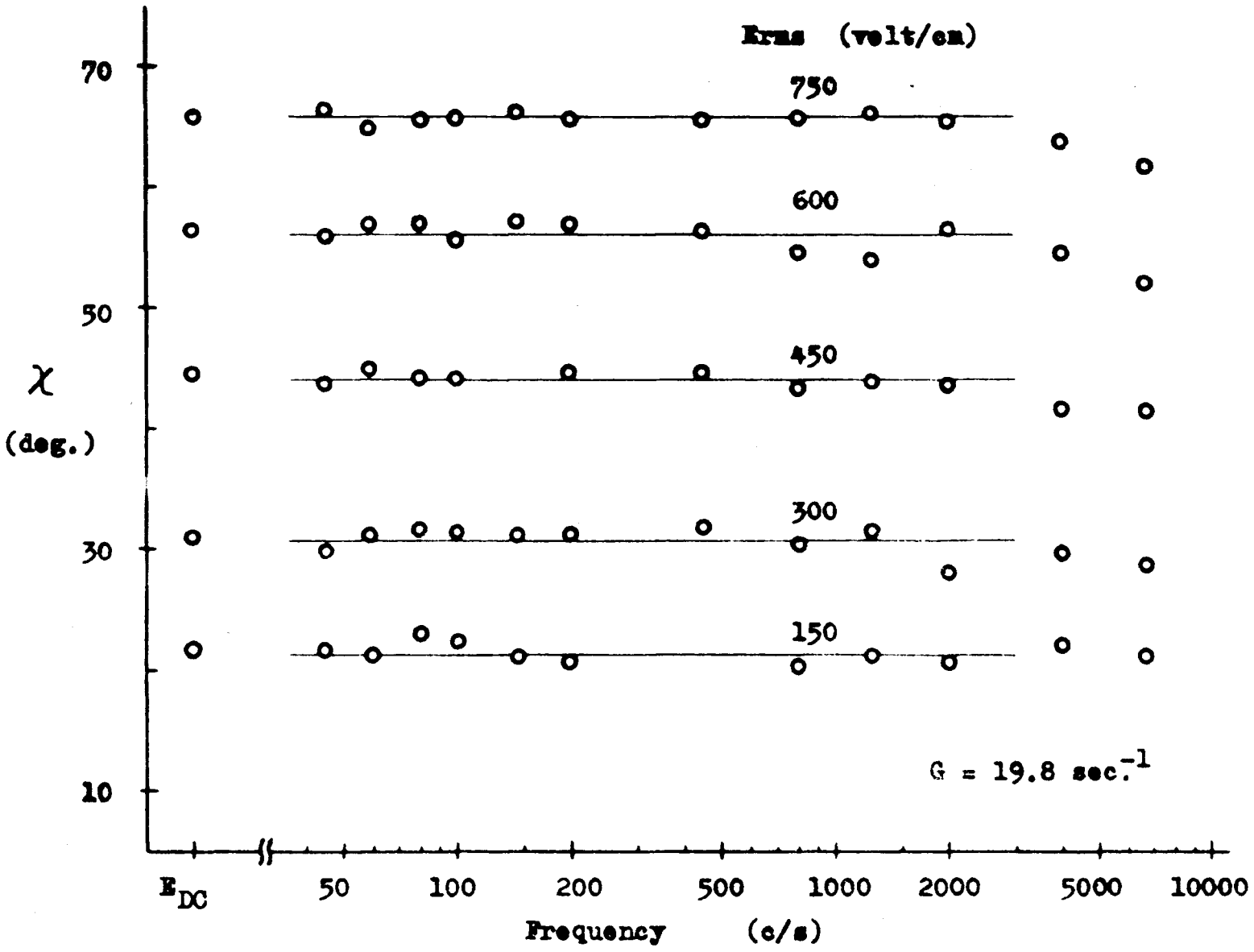

Fig. 4-7 Frequency Dependence of Extinction Angle in the Electric-streaming Birefringence of Yellow Bentonite in 95% Aqueous Glycol (0.033 w/v %)

V Discussion

Va Theoretical

The result of two dimensional treatment was found to be identical when E reduced to zero with the result obtained by Boeder in his theory of streaming birefringence. The final equation for the two dimensional extinction angle showed that when $E \neq 0$ and $G = 0$ the extinction angle should be 90° or 0°, corresponding to the sign of μ_a^2, which agreed with preliminary considerations and experimental results.

Then, the results of three dimensional theory were expected to be the analogous equation, being only different in the numerical value; that is, the denominator of the first term would be replaced with 6.

The calculation of generalized theory was carried out in comparison with the corresponding term in the two dimensional treatment.

i) Extinction angle

The final equation for the extinction angle shows that in the special case of $E = 0$ it is in complete agreement with the result of Peterlin and Stuart[17] for streaming birefringence, $\cot 2\chi = G/6\Theta + O(G^3) + \cdots\cdots$, though this equation was obtained by the series expansion with α, β, and γ, but not with R as done by them. Then, it will be concluded that in the given limited condition, Eq. (2-35) is quite adequate.

Eq. (2-35) also shows that the result of the qualitative treatment made by Tolstoi[18] is probable. Tolstoi obtained the relation, with the notation described here, the deviation of $\cot 2\chi$ by applied electric field,

$\Delta \cot 2\chi \sim E^2/G$, for the case of induced dipole orientation in an electric and a hydrodynamic field.

It should be noticed in the case of $\mu_a^2/R > 0$, the region of the extinction angle should be from 90° to 0°; and when the extinction angle decreases from 90°, the extinction angle at E = 0 also decreases with the same sense. Then, the definition of the extinction angle of electric-streaming birefringence should be described as already mentioned (page 4) for experimental use.

There are many relations derived from Eq. (2-35) to determine the value of μ_a, but some of them are not adequate.

The relations $\mu_a^2/R > 0$, $G_{\chi=45^\circ} = (6\mu_a^2/R)^{\frac{1}{2}} \oplus E/kT$ (Eq. (2-37)) or $\mu_a^2/R < 0$, $G_{\chi=max} = (-6\mu_a^2/R)^{\frac{1}{2}} \oplus E/kT$ cannot give so accurate results because of the uncertainty in determining the points $\chi = 45^\circ$ or χ = max. in χ-G plot, and also in determining the vale E at cot 2χ = 0 in cot 2χ $-E^2$ plot, when $\mu_a^2/R > 0$. (. (2-

The initial slopes in χ-G curves, Eq. (2-36), are also available for determining the μ_a value, but it would be erroneous, since it is not verified that the applied electric field, which is able to change the extinction angle at small G, is small enough.

These calculations, therefore, may be complemental ways.

For determining the μ_a value, it is most satisfactory to plot in the cot 2χ $-E^2$ coordinate, in which the contribution of electric field strength can be estimated, and then to calculate from the slopes with the relation $\partial(\cot 2\chi)/\partial(E^2) = -\oplus \mu_a^2/RG(kT)^2$ (Eq. (2-39)). The slopes will indicate the proper region of G values.

ii) Magnitude of Birefringence

Comparing Fig. 2-4 with Fig. 2-3, it can be seen that the change in the values of the ordinate with increasing G is less in the magnitude of birefringence than the extinction angle, at small E and G values.

Eq. (2-41) shows that if the macromolecule is isometric, R = 0, and/or isotropic, $(g_1-g_2) = 0$, no birefringence is exhibited. (Also, as the common feature of orientation birefringence, no birefringence is expected when $n = n_s$, where n_s is the refractive index of the solvent.)

In the special case of E = 0, Eq. (2-40) is in complete agreement with the result of Peterlin and Stuart for the streaming birefringence,[17] where

$$\Delta n = \frac{2\pi\phi}{n}(g_1-g_2)\frac{R}{15}\frac{G}{\Theta}\left\{1-\frac{1}{12}\left(\frac{1}{6}+\frac{R^2}{35}\right)\left(\frac{G}{\Theta}\right)^2+\cdots\right\} \qquad (5\text{-}1)$$

In the case of G = o, Eq. (2-40) is reduced to

$$\Delta n = \frac{2\pi\phi}{n}(g_1-g_2)\frac{1}{15}\left(\frac{\mu a}{kT}\right)^2 E^2\left\{1+\cdots\right\} \qquad (5\text{-}2)$$

which states Kerr's law.[12] [17]

Eq. (2-44) is the similar result of Tolstoi in the case of the induced dipole orientation of pure liquids.

From the value of Δn, it is generally impossible to find each value of Θ, μ_a and (g_1-g_2). When the values of Θ and μ_a are known from the extinction angle or other methods, the value of optical anisotropy factor (g_1-g_2) can be obtained. But it may be a complemental way.

There are more favorable methods to determine the value of

(g_1-g_2). One is the usual method from the values of streaming birefringence (E = 0) with Eq. (2-44) and another is the method from the values of electric birefringence (G = 0) with Eq. (2-43) since the line of Δn-E^2 plot at G = 0 is straight within the region of unsaturated, small E values.

The simple way to determine the values of Ⓗ, μ_a and (g_1-g_2) will be concluded that Ⓗ value is determined from the initial slope of χ-G plot at E = 0, and then μ_a value is determined from the slopes of cot 2χ -E^2 plot. (g_1-g_2) value is determined from the initial slope of Δn-G plot at E = 0 with the obtained Ⓗ value.

The optical anisotropy factor (g_1-g_2) is given by Peterlinc and Stuart[11] related with the axial ratio and each component of the polarizability can be separated by observing the refractive index increment.

Vb Experimental

i) On the results of electric-streaming birefringence of poly-γ-benzyl-L-glutamate with an electrostatic field

The conformation of PBLG in m-cresol has been reported to be the α-helix, which has a rod shape with the diameter 2b = 15 A and the length 2a = 1.5 A x PN (the number of polymerization of the constituent amino acids).

Since the molecular weight used in these experiments was found to be 206,000 as a viscosity average molecular weight, the average number of polymerization and the average lengths of PBLG α-helix are 940 and 1410 A, respectively.

Assuming PBLG in m-cresol is rigid under both an electric and a hydrodynamic field, and has a shape equivalent ellipsoid of revolution with an equatorial diameter 2b=18.3 A as treated by Doty et. al.,[15] the length of revolutional axis was calculated from the obtained rotational diffusion constants, 220 sec.$^{-1}$ at 21° C (η_s = 0.176 poise) and 420 sec.$^{-1}$ at 31°C (η_s = 0.092 poise) by means of Eq. (1-2). The length of revolutional axis was found to be 1680 A and 1700 A, respectively.

Since there was no difference in the measured extinction angles of two different concentration samples (0.243% and 0.127 %) within the experimental error, the obtained rotational diffusion constants and also the calculated lengths shall be adequate; but more precise experiments on concentration dependents of the rotational diffusion constant may result in different values, as shown by Yang.[19] The disagreement may be explained as follows: that the measured rotational diffusion constants with the streaming birefringence method should correspond to that of larger macromolecules which will be more easily orientated in a hydrodynamic field than shorter macro-

molecules when there is some extent of molecular weight (length) distribution. The sample of PBLG must have a molecular weight distribution. The calculation was done with Eq. (1-2) and with the assumption as an equivalent ellipsoid, which will result in a larger value of axial length as much as the value calculated with Burgers' Eq. (1-4), since the equivalent equation derived from Eq. (1-2) and the definition of an equivalent ellipsoid can be given approximately as

$$[\eta]_e = \frac{3\bar{\nu}kT}{8\pi\eta_s a^3}\left(\ln\frac{2a}{b} - 0.7\right) \qquad (5\text{-}3)$$

Eq. (5-3) closes to Eq. (1-4) which has been reported to result in larger values for lengths than that measured by other experimental methods.

Fig. 4-1 shows that the sign of μ_a^2/R is positive. Since it has been no objection to the elongated shape ($R > 0$) given for PBLG in m-cresol, the excess electric polarity (the direction of μ_a) can be determined to be coincident with the revolutional axis. It has been reported that PBLG has little electric polarizabilities even in a saturating electric field[7], so that the contribution of (g_1-g_2) on the μ_a value can be neglected.

Then, the calculated values 3200 D and 3110 D for the apparent electric parameter μ_a can be treated as the average values of permanent dipole moment μ_1^* along the axis of revolution of PBLG. The value of μ_1^* can be made equal to the value of μ_1, since the macromolecule is a very long rod. The residual permanent dipole moment is calculated with dividing by 940 and is found to be 3.4 D and 3.3 D, which agrees satisfactorily with the value usually assigned to a peptide bond moment and that estimated by other methods, such as saturating electric birefringence[7], the dielectric dispersion[20], and the light scattering in an electric field[21].

The calculation of the μ_a value with Eq. (2-36) from Fig. 4-1 was tried, but the values of velocity gradient at $\chi = \pi/4$ on each curve could only obtain with large errors. The calculation of μ_a value with Eq. (2-36) from Figs. 4-2 and 4-3 was also tried and it was found that the values from each intersecting point at cot $2\chi = 0$ had larger distribution than the values obtained from the slopes. It will come from the experimental and theoretical (Eq. 2-35) inaccuracy and the molecular weight distribution.

It will be pointed out that the latter two ways for determining μ_a value are not so appropriate when χ-G curves obtained with small angles of inclination at $\chi = \pi/4$, and these ways will be complemental methods to support the obtained μ_a value from slopes in cot 2χ -E^2 plots.

In Figs. 4-2 and 4-3, it is shown that the higher electric field the larger the deviation from the linear relation occured. These phenomena will come mainly from the electrical effects such as polarization of solvent which will lower the effective electric field strength applied on PBLG.

Results of transmitted light intensity measurement show the similar tendency with the theoretical curves.

The intensity I of transmitted light through the annular gap is given

$$I = A\, I_0 \sin^2 \frac{\delta}{2} \qquad (5\text{-}4)$$

where $A = \sin^2 2\rho$, constant, in which ρ is an angle between an axis of birefringent fluid and the axis of the polarizer. I_0 is light intensity when two axes of polarizing filters are parallel without any external field. And

$$\delta = 2\pi l \Delta n / \lambda_0 \qquad (5\text{-}5)$$

where λ_o is the wave length of monochromatic filter (546 mμ), and l is the optical path in the birefringent field, and Δn is the magnitude of birefringence.

Without any external field, the deflection of the oscillograph was calibrated with whole angle θ (90^0-0^o) between axes of polarizing filters and obtained the good relation $I=I_o\cos^2\theta$. Then the light intensity was measured and each value was substituted as an equivalent angle θ , so that the ordinate scale in Fig. 4-4 should correspond to the magnitude of birefringence.

At zero velocity gradient the intensity shows fairly good relation of Kerr's law. But the curves exhibit neither monotonous increase nor horizontal initial slopes.

These disagreements will be explained by the following reasons: Halo was observed around the photographed annular gap when an electric field was applied. The halo came from not only hallation, but also mainly the scattering light from the annular gap. The intensity of scattering light which can lower the transmitted light intensity was generally observed to be more intense with increasing DC field, and less with increasing hydrodynamic field. The curves in Fig. 4-4 correspond to these observations from photographs. The minimum points in the curves will show that there will be the maximum point relating to the two field strengths where the turbulence of the laminarly streaming solution is maximum: the solution under experiments was tinged after repeating application of DC field, and the absorbance of green light (546 mμ) by the orange-yellowish solution led to some amount of experimental error on the transmitting light intensity measurements.

To avoid unexpected effects of electric field on the solution, a transmitted light intensity measurement as weill as a photographing method should

be replaced to the usual method of birefringence measurement in order to minimize the duration of electric field application. The results, however, are not so satisfactory that no more improvement is needed.

ii) On the results of electric-streaming birefringence of yellow bentonite with an electrostatic field

Since the shape of yellow bentonite is a flat disc ($R<0$), as seen by the electronmicroscopy[22], and from Fig. 4-5 (a) the sign of μ_a^2/R is found to be positive, the sign of μ_a^2 can be determined to be negative. Then the excess electric polarity lies in the plane of disc. It will be natural to concern that these flat clay had a multi-lamellar structure of silicate, and has negligible electric moment along the direction perpendicular to the plane of disc.

The values of the rotational diffusion constant indicate the sample is largely heterogeneous. Neither the average diameter of yellow bentonite disc (e.g. $\Theta = 1.5$ corresponds to 1800 A.) nor the value of apparent electric parameter (e.g. in the order of 10^5 D) can be estimated.

And in these experiments, the identical slopes of cot 2χ -E^2 plots were obtained with the different velocity gradients (Fig. 4-5 (b)). The curious feature of cot 2χ -E^2 plots comes from the large conductivity of the 95% aqueous glycol suspension of yellow bentonite (the ohmic resistance was measured between two cylinders and found to be less than 500 ohm.). The addition of glycol to lower the conductivity without harm was affected to the Θ value resulting too large, and which is also the reason for the accidental curious feature of these results.

iii) On the results of electric-streaming birefringence of poly-γ-benzyl-L-glutamate with an alternative electric field

Because of the sensitive deviation of extinction angle with an electric field and of satisfactory large deviation with 3000 V/cm. electric field, the frequency dependence of extinction angle was measured with AC of 300 Vrms.

The results obtained in the dispersion study (Fig. 4-6) shows typical dispersion curves. At the sufficiently low frequency (less than 100 c/s), PBLG molecules will rotate according to the change of the voltage and the direction of applied sinusoidal electric potential, so that the deviation of the extinction angle will fluctuate and also there should be some amount of turbulence on the laminarly streaming solution; there will be the reason of difficulty in measurements of extinction angle at low frequencies.

With increasing frequency there will be increasing difficulty in following to the alternative field, since PBLG has only a permanent dipole moment along the axis of revolution. [7] At a sufficiently high frequency PBLG has little chance to follow the field and there is no deviation on the extinction angle by the electric field.

There was another reason to call these phenomena the permanent dipole orientation dispersion. With the photomultiplier attachment the transmitted light intensity was also observed; it was found that the intensity deviated with a given frequency and decreased with increasing frequency.

When the results in Fig. 4-6 are replotted in the coordinate of percent deviation of cot 2χ with frequency against the applied frequency, Fig. 5-1 can be obtained. The values obtained with different velocity gradients are on the same curve without some deviation at low frequency. It is also found that the 50% change frequency (say, "the critical frequency") is 300 c/s.

If the dispersion theory of Debye [23] can be applied on this plot, a

solid curve shown in Fig. 5-1 will be available. The formula is

$$\frac{\Delta \cot 2\chi}{\cot 2\chi_{E_{DC}} - \cot 2\chi_{E=0}} = \frac{1}{1+\omega^2\tau^2} \qquad (5\text{-}6)$$

where

$$\Delta \cot 2\chi = \cot 2\chi_f - \cot 2\chi_{E=0}$$
$$\cot 2\chi_{f=\infty} = \cot 2\chi_{E=0}$$
$$\cot 2\chi_{f=0} = \cot 2\chi_{E_{DC}}$$

and where ω is the angular velocity of applied electric field ($= 2\pi f$) and τ is the relaxation time of PBLG ($= 1/2\Theta$). The solid curve does not show the most probable curve on the obtained results. From the critical frequency, the rotational diffusion constant of PBLG can be found to be 940, which corresponds to the length of revolutional axis of 1270 A. The value is smaller than the viscosity average length.

The discrepancy will come from the distortion of applied sinusoidal wave and the excess effective voltage of applied field (in Figs. 4-2 and 4-3, 3000 V_{DC}/cm results are out of the linear relation), and the difficulty of measurements at low frequency and also the polydispersity of PBLG sample.

The smaller value will be explained mainly by the polydispersity of PBLG, since a smaller PBLG will orientate more easily than a larger one under the AC field and the constant velocity gradient.

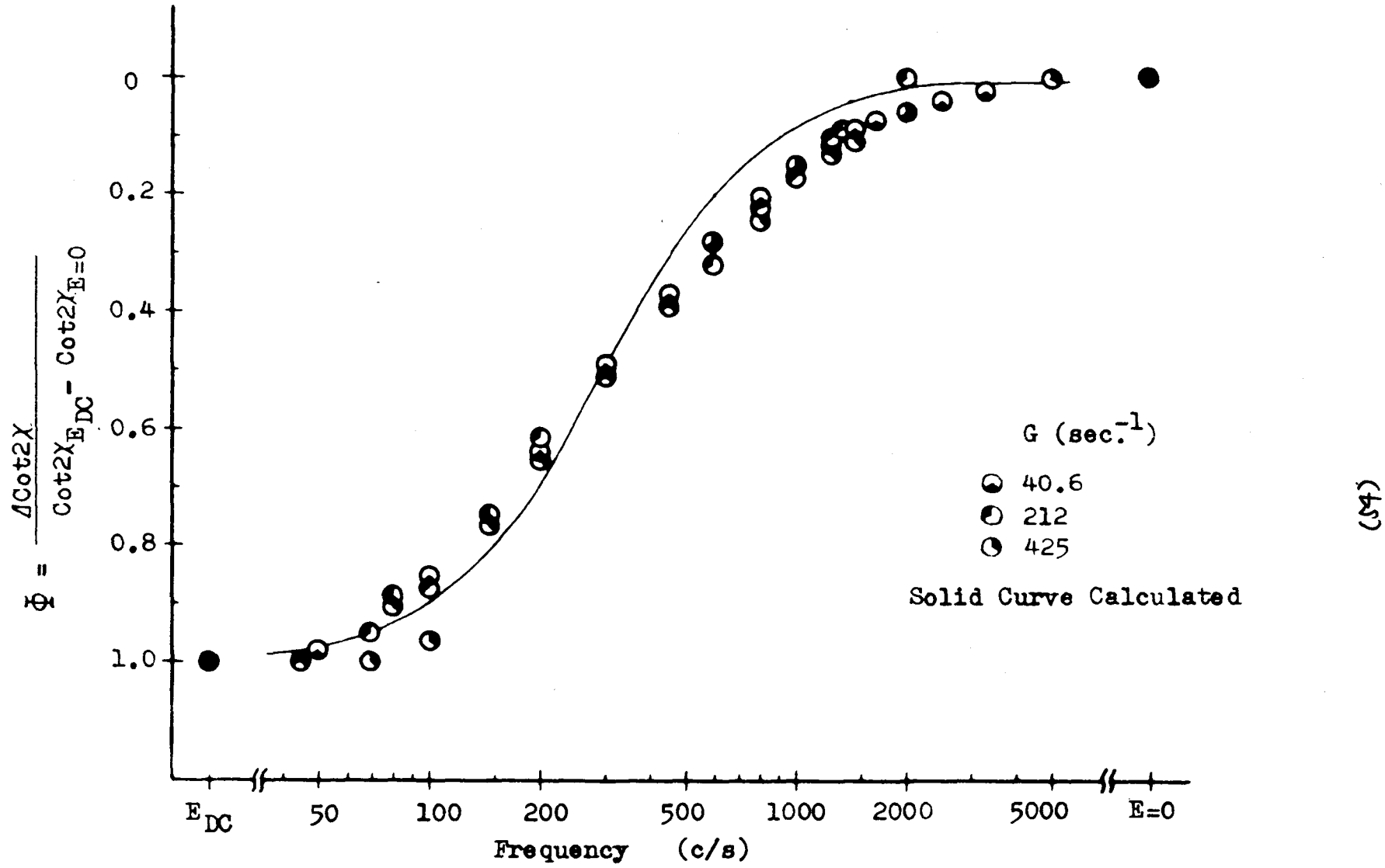

(34)

Fig. 5-1 Frequency Dependence of Cot 2χ in the Electric-streaming Birefringence of PBLG (T-629) in m-cresol

iv) On the results of electric-streaming birefringence of yellow bentonite with an alternative electric field.

As expected from the nature of yellow bentonite, the results of the dispersion study showed no frequency dependence. The deviation of extinction angle are constant at a given effective voltage of applied field all over the examined frequency. And the relation of cot $2\chi_{f=\theta} = \cot 2\chi_{E_{DC}}$ was confirmed fairly well. The fluctuation of the values lower than 3 kc/s will come from the large conductivity of suspension and that of the values higher than 3 kc/s will come additionally from the distortion of the applied sinusoidal waves.

If the bentonite disc has a permanent dipole moment, the extinction angle must decrease at least within some 10 c/s concerning with the rotational diffusion constants. The absence of permanent dipole moment in yellow bentonite was supported by the transmitted light intensity measurements on the oscillograph, where the frequency of incident light signal was twice as high as the applied frequency and the amplitude changed in an analogous manner as described by O'Konski et al. [8] Moreover, the frequency of 3 kc/s is too low to concern the decreasing phenomena as a dispersion caused by the retardation of induced dipole formation.

It can be concluded that the yellow bentonite has only an electrical polarizability and the larger polarizability lies in the plane of the bentonite disc ($g_{e2} > g_{e1}$).

Vc Miscellaneous

It was already shown that the extinction angle is most easy to measure and also more sensitive to the applied fields. The photographic method employed in the extinction angle measurement is better than the usual naked-eye method [24] [25] in minimizing experimental error and duration, which can reduce the influence of temperature change and external fields, since these effects were found to increase with the applying duration of external fields.

The transmitted light intensity measurement should be improved and there will be a method proposed by Zimm [26] or a method to measure the light intensity coming from a small part of the annular gap with the aid of a quarter wave plate.

The AC method appeared to be better than the DC method for the following reasons: 1) fewer effects such as polarization, electrophoresis, and/or electrolysis are expected with the AC method; 2) by extrapolating the frequency to zero, the value corresponding to the identical effective DC field can be obtained; 3) a power source can be more easily designed for the AC method than for the DC method. It may be possible to use cylinders coated with barium titanate [16] in the case of highly conductive solutions. The measurements of frequency dependence will result the illustration for the sort of electrical moment that lies in the examined macromolecule. It will be interesting to observe the change in the size and shape and/or the value of induced dipole moment with the change of the circumstance and/or the nature of the biological macromolecule, as done by Takashima and Lumry [27] on the change in the value of permanent dipole moment and relaxation time of haem-protein. Tinoco [28] observed the change in the electrical properties of

fibrinogen on its activation by pH change with the electric birefringence method.

If Eq. (5-6) shows the true nature of dispersion phenomena, the following empirical equation will be available:

$$\cot 2\chi = \frac{G}{6\Theta} - \frac{\Theta}{RG}\left[\frac{(g_{e1}-g_{e2})}{kT} + \frac{1}{1+\omega^2\tau^2}\left(\frac{\mu_i^*}{kT}\right)^2\right] E_{rms}^2 \qquad (5\text{-}7)$$

If the macromolecule has both permanent and induced dipoles, the dispersion curve of the extinction angle will change with increasing frequency from the steady value corresponding to E_{DC} to the other steady value corresponding to the induced dipole orientation (but not equal to the value at $E = 0$). However, this problem is expected to be solved theoretically based on Eqs. (1-5) and(2-25) at $\partial f/\partial t \neq 0$.

If the measurement with a high frequency AC field were possible, the dispersion phenomena would be observed with a sample only carrying induced dipole, in respect to the retardation of induced dipole formation.

The AC method will be utilized also to estimate the flexibility and/or the size and shape distribution of macromolecules of the same species.

In Fig. 5-2, a modified assembly of concentric cylinders is tentatively proposed. In particular, the space where the image of the annular gap is interfered by the inner cylinder holder is used as the system for transmitted light measurement. The system -- the Senarmont compensator system [29] -- is the same as that in electric birefringence [30], so that the extinction angle by photographing and the magnitude of birefringence by the system and recorder can be measured simultaneously and rapidly. The adjuscent temperature jacket is designed to be in both uses for thermostatting and lubricating. It may be possible that some temperature control

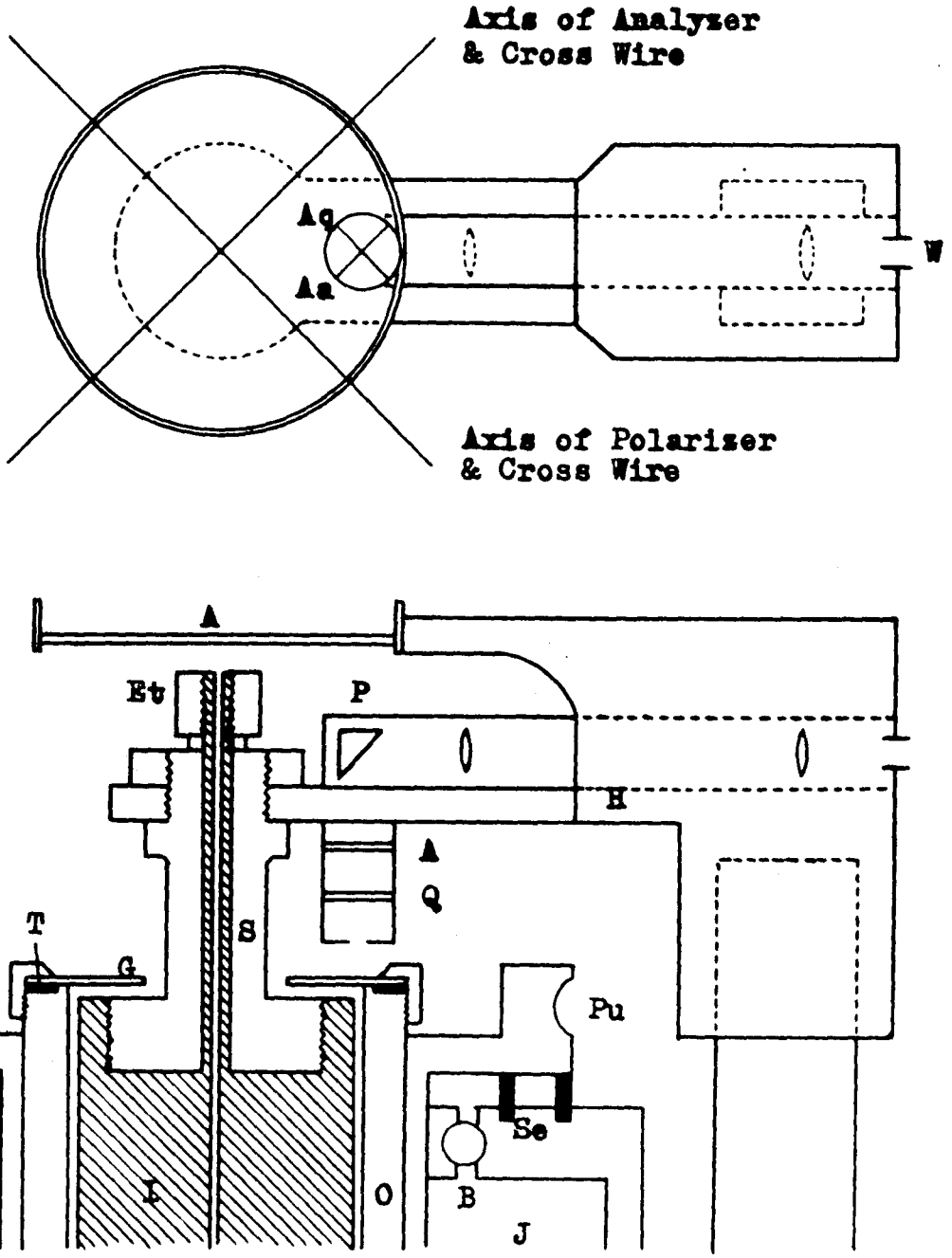

Fig. 5-2 A Cross-sectional Sketch of Cylinder Assembry for Electric-streaming Birefringence Apparatus

I: insulated stationary inner cylinder, O: grounded rotatory outer cylinder, S: insulating stem of inner cylinder, Et: electrode terminal, G: glass window, T: teflon packing, Bs: brush shoe, Se: seal, J: jacket, B: bearing, Pu: pulley, H: inner cylinder holder, Q: quarter wave plate, A: analyzer, P: prism, Aq: axis of quarter wave plate, Aa: axis of analyzer, W: window to a photomultiplier circuit.

system is built in the inner cylinder.

Since the distribution function of the macromolecular axes under the influence of two externally applied fields is solved. The effect of the electric field on the non-Newtonian viscosity will also be solved with the distribution function.

VI Conclusion

The electric-streaming birefringence method presented here appears to be a good technique for determining the rotational diffusion constant and the electrical and optical properties of macromolecules simultaneously.

The theoretical basis of the method is in accord with the theory given by Peterlin and Stuart in the extreme cases of either an electric field or a hydrodynamic field being zero.

The experimental results calculated on a basis of the theoretical arguments presented here are in excellent agreement with those reported using other methods in the case of measurements with an insulating medium. The results suggest, however, in the case of measurements with a conductive medium, that it will be necessary to improve the method.

The method using an alternating electric field together with a hydrodynamic field will be further developed as a very simple method for determining individually the permanent and induced dipole moments in a macromolecule.

VII ACKNOWLEDGMENTS

The author wishes to send his hearty thanks to Professor Shiro Akabori for his powerful encouragement and to Professor Toshizo Isemura for providing the facilities to pursue this research and for his encouragement and discussions.

The author also thanks Professor Hiroshi Fujita and Professor Shiro Takashima for their discussions and Dr. Shoichi Ikeda for his discussions and assistance with the mathematical treatment of the theory.

VIII REFERENCES

(1) Perrin J. Compt. rend. 149, 549 (1909)

(2) Einstein A. Ann. Phys. (4) 17, 549 (1905), 19, 371 (1906)

(3) Perrin F. J. phys. radium (7) 5, 497 (1934)

(4) Gans R. Ann. Phys. (4) 86, 628 (1928)

(5) Burgers J. M. Kon. Ned. Akad. Wet., Verhand. 16, 113 (1938)

(6) Broersma S. J. Chem. Phys. 32, 1626 (1960)

(7) O'Konski C. T., K. Yoshioka & W. H. Orttung
J. Phys. Chem. 63, 1558 (1959)

(8) O'Konski C. T. & A. J. Haltner J. Am. Chem. Soc. 79, 5634 (1957)

(9) Boeder P. A. Physik 75, 258 (1932)

(10) Jeffery G.B. Proc. Roy. Soc. London (A) 162, 161 (1922)

(11) Peterlin A. & H. A. Stuart Hand- & Jahrbuch der Chem. Phys. (Leipzig)
8, IB (1943)

(12) Kerr J. Phil. Mag. 50, 337, 446 (1875); 8, 85, 229 (1879);
13, 53, 248 (1882); 37, 380; 38, 144 (1884)

(13) Isemura T. & Y. Mukohata Symposium on Bio-phys. chem. 5, 74 (1960)
(in Japanese)

(14) Rao Instruction manual (1959)

(15) Doty P., J. H. Bradbury & A. H. Holtzer
J. Am. Chem. Soc. 78, 947 (1966)

(16) Mukohata Y. unpublished

(17) Peterlin A. & H.A. Stuart Z. Physik 112, 1, 129 (1939)

(18) Tolstoi N. A. Doklady Akad. Nauk. SSSR 59, 1563 (1948)

(19) Yang J. T. J. Am. Chem. Soc. 80, 5139 (1958)

(20) Wada A. J. Chem. Phys. 30, 328 (1959)

(21) Wallach M. L. & H. Benoit J. Polymer Sci. 57, 41 (1962)

(22) Isemura T. & Y. Mukohata Nippon Kagaku Zasshi 80, 657 (1959) (in Japanese)

(23) Debye P. Polar Molecule, Reinhold (1929)

(24) Edsall J. T., A. Rich & M. Goldstein Rev. Sci. Instr. 23, 695 (1952)

(25) Janeschitz- Kriegle H. Ibid. 31, 119 (1960)

(26) Zimm B. H. Ibid. 29, 360 (1958)

(27) Takashima S. & R. Lumry J. Am. Chem. Soc. 80, 4238, 4244 (1958)

(28) Tinoco I. Jr. Ibid. 77, 3476 (1955)

(29) de Senarmont Ann. chim. phys. 73, 345 (1840)

(30) Benoit H. Ann. phys. 6, 561 (1951)